Applications of Photodetectors in Particle Physics and Medical Imaging

Craig Woody

Physics Department

BROOKHAVEN NATIONAL LABORATORY

Short Course on Advanced Photodetectors

2010 Nuclear Science Symposium and Medical Imaging Conference

October 31, 2010

IEEE

NUCLEAR & PLASMA SCIENCES SOCIETY

Outline

- Introduction
- Principles of photon detection
- Review of design considerations for photon detectors
- Applications
  - High energy and nuclear physics
  - Medical imaging

What is a Photodetector ?

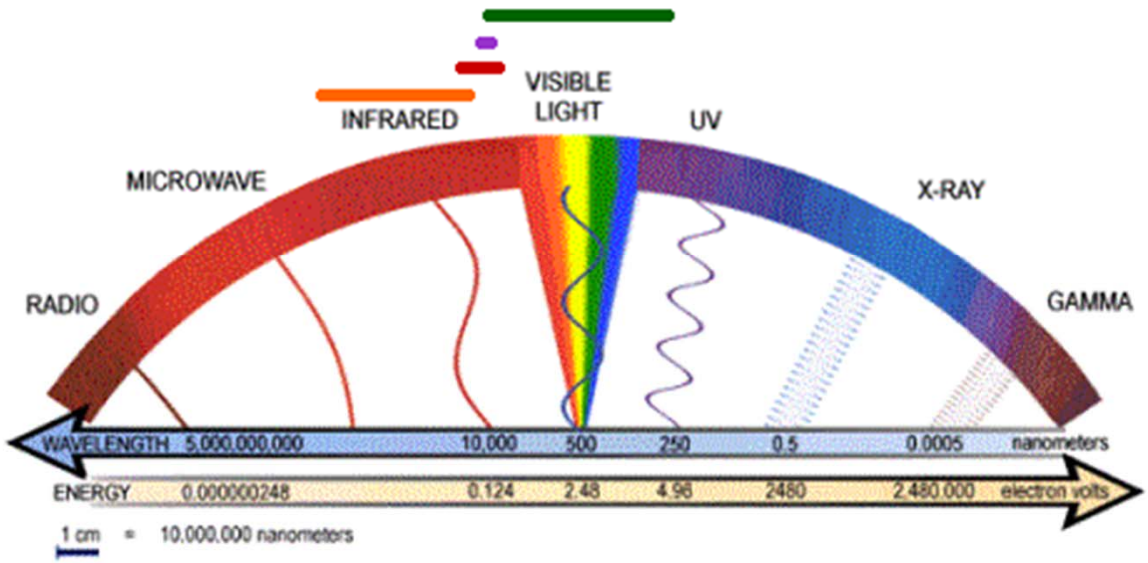

- Purpose of a photodetector is to detect photons
- However, the energy range of photons that we wish to detect is extremely large:

  < 0.1 eV ~ $> 10^{14}$ eV (>100 TeV)
- This requires many *different* kinds of photodetectors

Photodetectors vs Photon Detectors

- Define a photon detector as a device that detects photons of an arbitrary energy
- High energy photons (E > 1 MeV) are very penetrating and require high stopping power
- Define a photodetector as a device that detects photons in the eV to few keV range (IR to X-ray). These photons may be detected directly or may be produced by some other type of photon detector

Photon Interactions in Matter

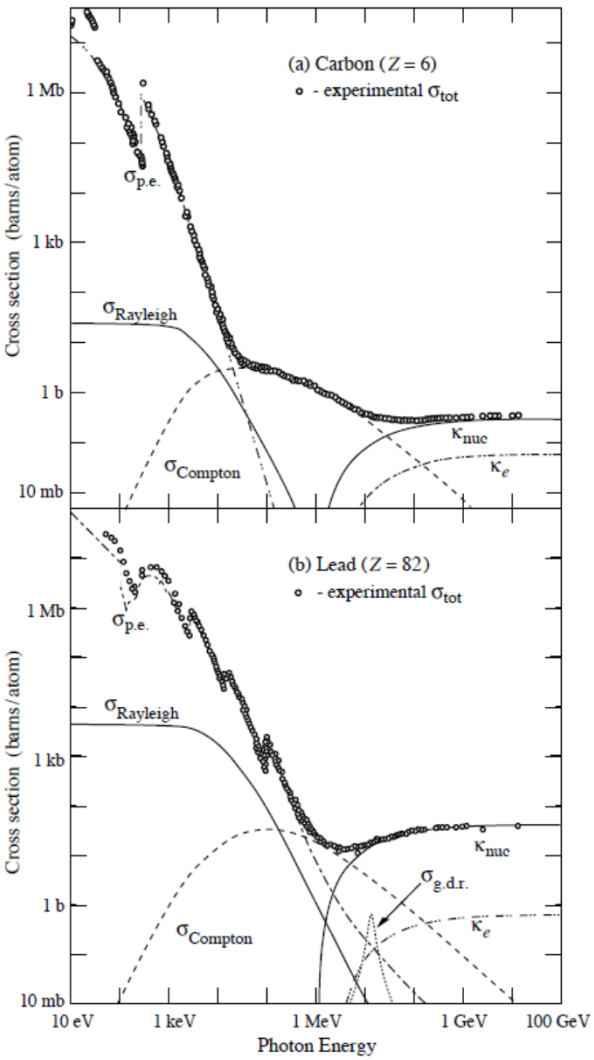

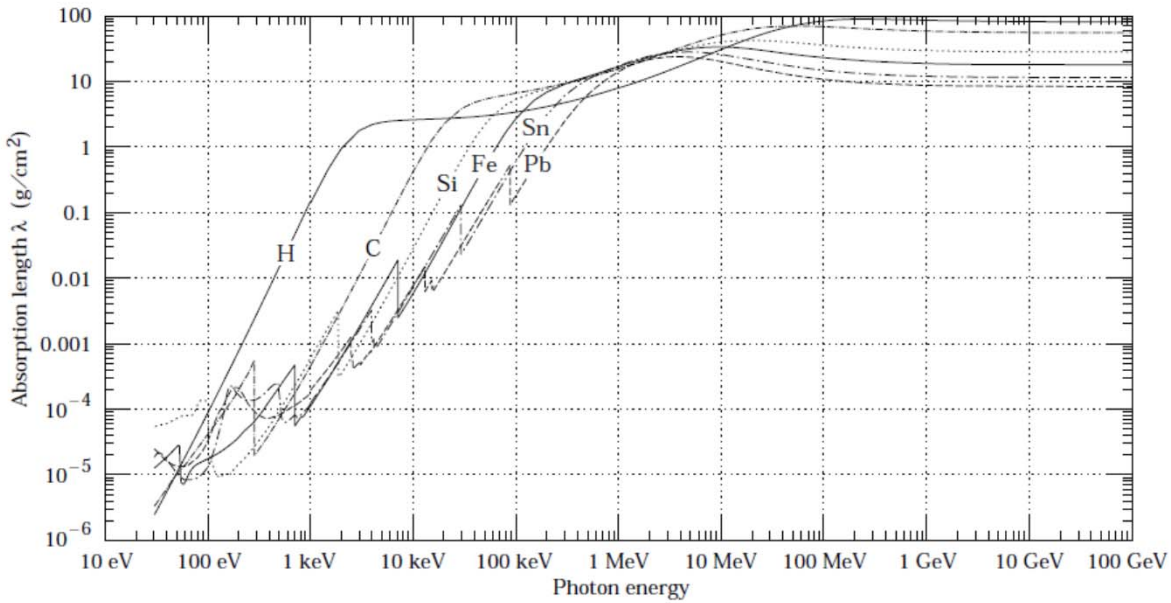

Inverse Attenuation Length $\mu = \rho/\lambda$ (cm^{-1}) $I(x) = I_0 e^{-\mu x}$		
E	Si	Pb
10 keV	93.2	1419
1 MeV	0.15	0.67
1 GeV	.08	1.34

Photon detection

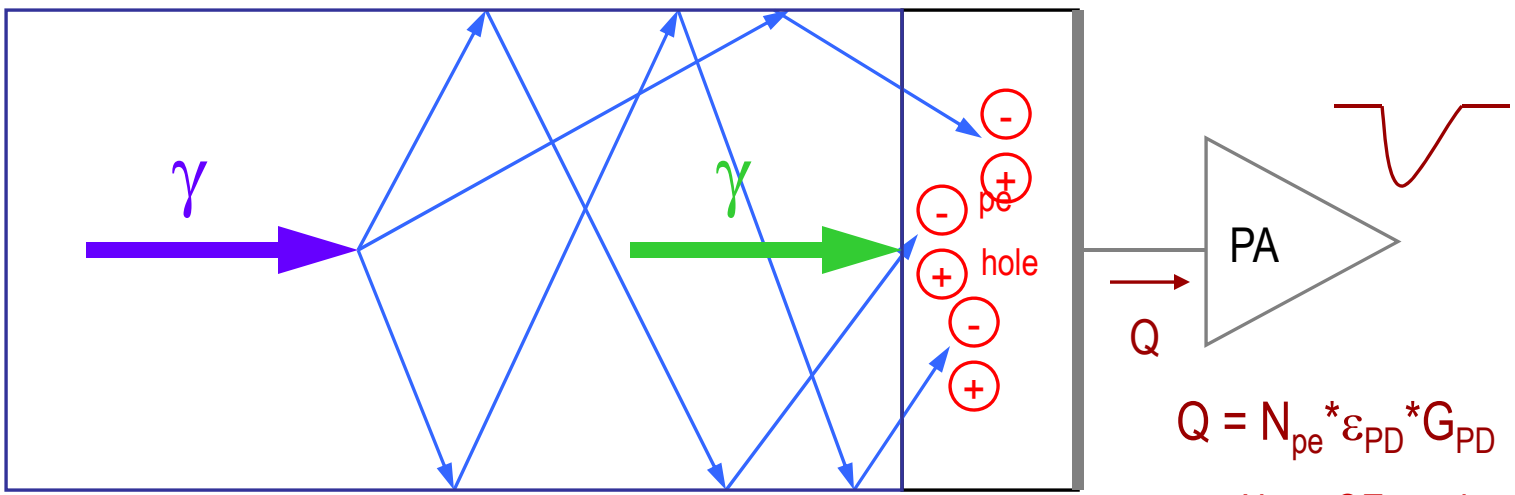

$Q = N_{pe} * \varepsilon_{PD} * G_{PD}$

Note: QE can be >1

$E_{e\text{-}h} = 3.62$ eV in Si

Gamma converter

Photodetector

Low energy γ interacts directly in photodetector producing *photoelectrons*

$$N_{pe} = N_{\gamma} * QE$$

High energy γ interacts directly in converter material and produces optical photons

$$N_{opt} = N_{\gamma} * \varepsilon_{con} \qquad N_{pe} = N_{opt} * \varepsilon_{col} * QE$$

Photoelectrons and Noise

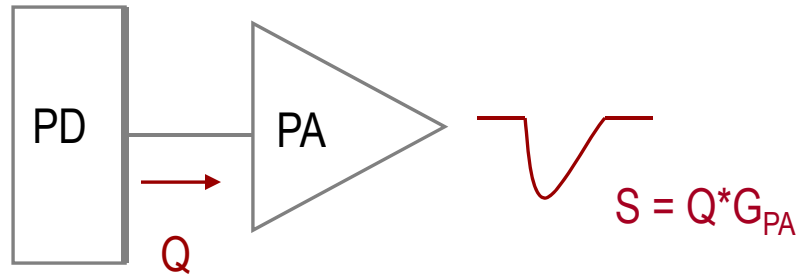

$N_{pe} = N_{\gamma} * QE$ $\qquad$ $Q = N_{pe} * \varepsilon_{PD} * G_{PD}$

Photoelectrons are the primary signal and can never be recovered at a later stage in signal processing

Figure of Merit : N_{pe}/MeV

$$\frac{\sigma(E)}{\langle E \rangle} = \sqrt{\frac{f_N}{N_{pe} \cdot \varepsilon_{PD}} + \left(\frac{ENC}{N_{pe} \cdot \varepsilon_{PD} \cdot G_{PD}} \right)^2}$$

f_N = Excess noise factor from photodetector

ENC = Equivalent Noise Charge in electronic gain stage

Low noise amplification at the early stage of signal processing is crucial for achieving good signal to noise

Photodetectors

Type	λ (nm)	$\epsilon_Q\,\epsilon_C$	Gain	Risetime (ns)	Area (mm^2)	1-p.e noise (Hz)	HV (V)	Price (USD)
PMT*	115–1700	0.15–0.25	10^3–10^7	0.7–10	10^2–10^5	10–10^4	500–3000	100–5000
MCP*	100–650	0.01–0.10	10^3–10^7	0.15–0.3	10^2–10^4	0.1–200	500–3500	10–6000
HPD*	115–850	0.1–0.3	10^3–10^4	7	10^2–10^5	10–10^3	$\sim 2 \times 10^4$	$\sim$600
GPM*	115–500	0.15–0.3	10^3–10^6	$O(0.1)$	$O(10)$	10–10^3	300–2000	$O(10)$
APD	300–1700	$\sim$0.7	10–10^8	$O(1)$	10–10^3	1–10^3	400–1400	$O(100)$
PPD	320–900	0.15–0.3	10^5–10^6	~ 1	1–10	$O(10^6)$	30–60	$O(100)$

Review of Particle Physics
Journal of Physics G, Vol 37, No 7A (2010)

PMT = Photomultiplier tube (workhorse, but doesn't work in magnetic fields)
MCP = Multichannel Plate Detector (dense, small diameter charge amplifiers - fast)
HPD = Hybrid Photodiode Detector (vacuum PMT with silicon sensor)
GPM = Gaseous Photon Detector (solid & gaseous photocathode – can cover large areas)
APD = Avalanche Photodiode (also PIN diode)
PPD = Pixellated Photon Detector (SiPM, GPMT, MPPC,…)

Matching the Photodetector to the Gamma Converter

Emission Weighted Quantum Efficiency: $\overline{QE} = \int QE_{PD}(\lambda) \cdot I_{em}(\lambda) d\lambda$

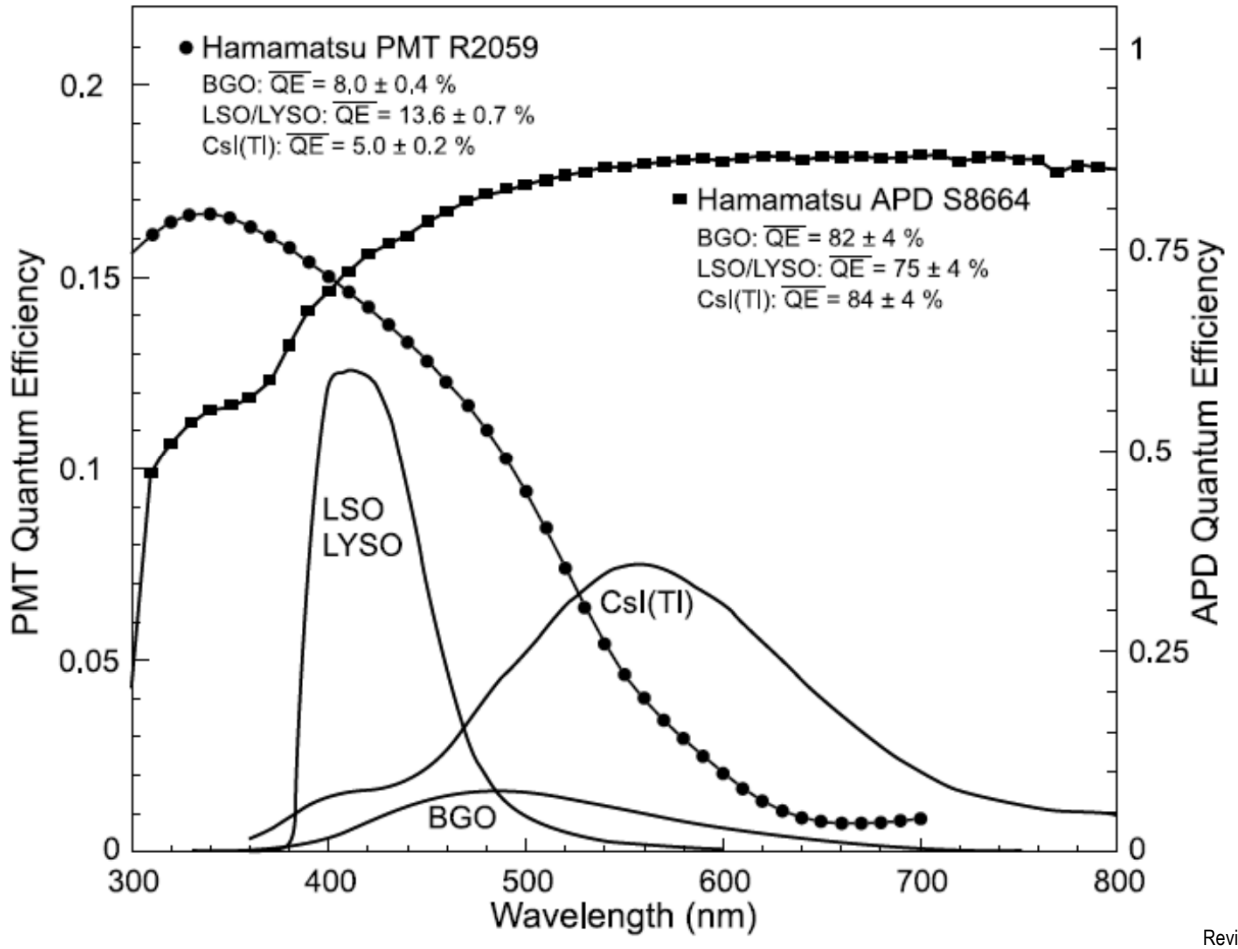

Review of Particle Physics
Journal of Physics G, Vol 37, No 7A (2010)

Gamma Converters

- Plastic Scintillators
  - Low density
  - Requires interspersing high Z absorber material to achieve high stopping power for high energy γ's

    Sampling technique $\Rightarrow$ Novel readout schemes
- Crystal Scintillators
  - High density and high Z
  - Leads to homogeneous detectors with very good energy resolution
  - Requires good light collection
- Noble Liquids
  - Moderate density and Z
  - Produce ionization plus scintillation
  - Requires working at cryogenic temperatures
- Cherenkov Materials
  - Possible high density (PbGl, PbF_2,…)
  - Relatively low light output

Plastic Scintillators

Review of Particle Physics
Journal of Physics G, Vol 37, No 7A (2010)

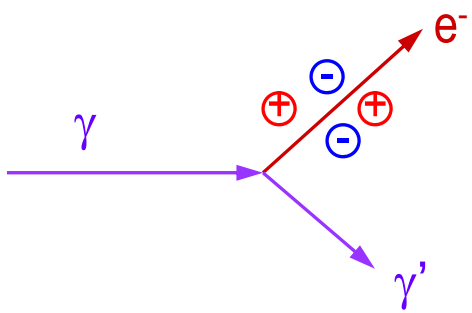

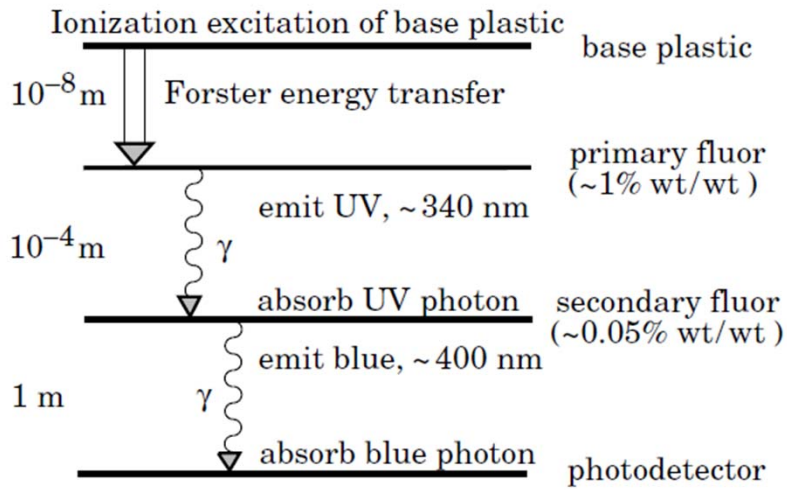

Gammas interact and produce electrons which cause ionization and excitation of the medium

- Primary ionization causes excitation of molecules in the base plastic
  - typically an aromatic compound such as polystyrene (PS) or polyvinyltoluene (PVT), or an acrylic compound such as polymethylmethacrylate (PMMA)
- De-excitation of the base plastic produces scintillation photons in the short wavelength UV (~ 300 nm), which are absorbed by a primary fluor, or energy is transferred directly from the base to the fluor in a very short distance.
- Primary fluor emits at a longer wavelength (~ 340 nm), which is absorbed by a secondary fluor that emits in the visible (~ 400 nm)
- Each process involves losses due to the efficiency of energy transfer at each step, resulting in an overall light yield of ~ 1 photon per 100 eV of energy deposit

Commonly Used Plastic Scintillators

Scintillator	Light output (% Anthracene)	Decay time (ns)	Wavelength of emission max (nm)	Attenuation length (cm)	Application
BC 400	65	2.4	423	250	General purpose
BC 404	68	1.8	408	120	Fast counting
BC 408	64	2.1	425	380	Large area
BC 412	60	3.3	434	400	Large area
BC 418	67	1.4	391	100	Ultrafast timing
BC 428	50	12.0	490	330	Green emitting

Bicron/Saint-Gobain

Review of Particle Physics
Journal of Physics G, Vol 37, No 7A (2010)

Light output of Anthracene ~ 20,000 γ/MeV (~ ½ of NaI)

Scintillator Non-Proportionality

Plastic scintillators do not responds linearly to ionization density

Saturation effects occur due to quenching and recombination

dE/dx ~ 2 MeV/cm for minimum ionizing particles

Semi-emperical formula:

Birks Law

$$\frac{dL}{dx} = L_0 \frac{dE/dx}{1 + k_B dE/dx}$$

k_B = Birks' constant
determined by measurement

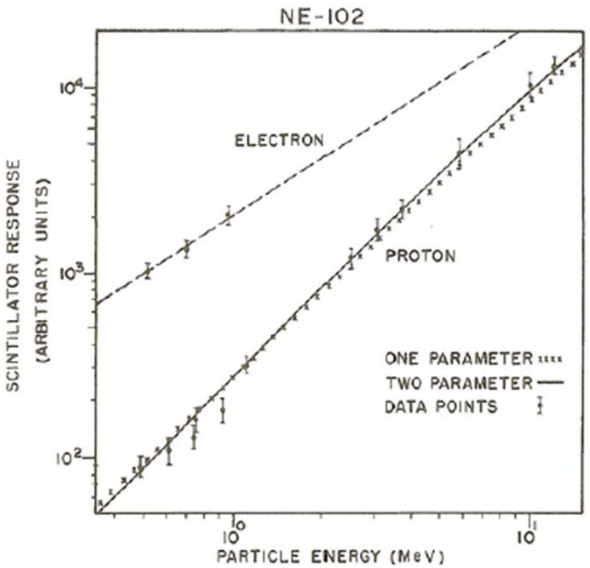

G.Knoll, Radiation Detection and Measurement

Wavelength Shifters

Wavelength shifters absorb light at a short wavelength and re-emit at a longer wavelength.

Change in wavelength between absorption and re-emission is called the Stokes Shift

Wavelength shifting can take place in the base plastic scintillator, or can be applied to the light produced by the scintillator using other materials such as wavelength shifting bars or fibers.

Wavelength shifting can accomplish several goals:

1. Improve light propagation in the material
   - Attenuation length of most base materials is much longer at longer wavelengths
2. Redirect the light for better light collection
3. Provide a better wavelength match to the photodetector

These features come at some cost:

1. Efficiency of wavelength shifting may be low
2. Primary light must be collected by the wavelength shifter
3. Decay time of wavelength shifter may be slower than primary emitter

Wavelength Shifters

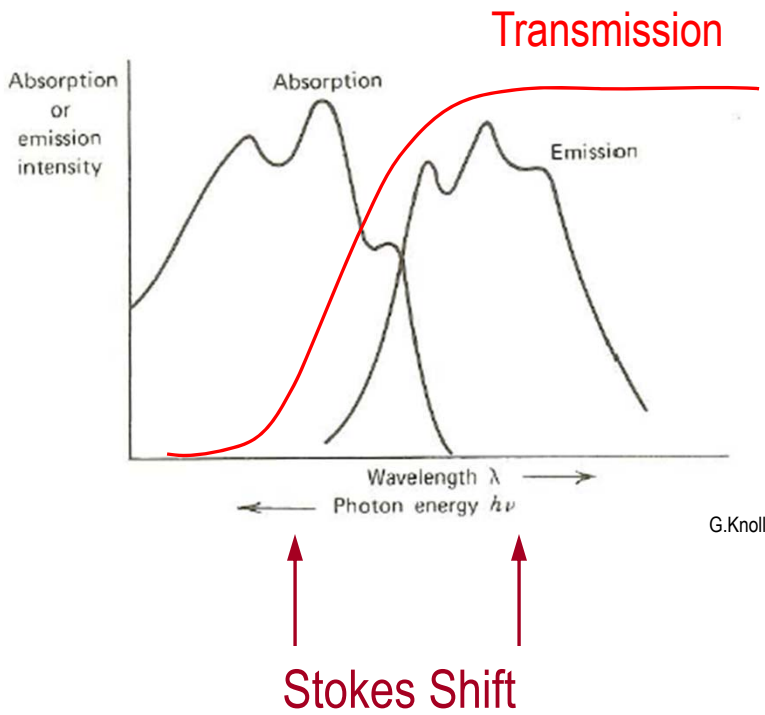

G.Knoll, Radiation Detection and Measurement

Longer Stokes Shift ⇒

- Better transmission at longer wavelengths
- Less self absorption

Crystal Scintillators

Crystals can be either natural scintillators or require an activator

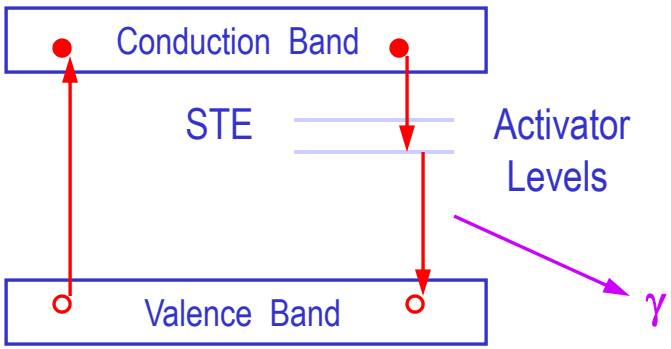

Scintillation Efficiency

$$\eta = \beta \cdot S \cdot Q$$

β = efficiency of energy conversion
S = efficiency of energy transfer to luminescent center
Q = efficiency of luminescent center to emit a photon

- Activators (Tl, Ce,…) create electronic levels in the forbidden gap
- Primary ionization excites an electron from the valence band to the conduction band, leaving a hole in the valence band
- Electron in the valence band forms loosely bound state with hole (Self Trapped Exiton) which moves freely through the lattice until it is captured on an activator site
- Activator then decays emitting a scintillation photon
  – determines wavelength and decay time

η depends strongly crystal
η ~ 0.5 for NaI(Tl) because Q ~ 1

Crystal Scintilators

Parameter:	ρ	MP	X_0^*	R_M^*	dE^*/dx	λ_I^*	τ_{decay}	λ_{max}	$n^\natural$	Relative output†	Hygro-scopic?	$d(\text{LY})/dT$
Units:	g/cm^3	°C	cm	cm	MeV/cm	cm	ns	nm				%/°C‡
NaI(Tl)	3.67	651	2.59	4.13	4.8	42.9	230	410	1.85	100	yes	−0.2
BGO	7.13	1050	1.12	2.23	9.0	22.8	300	480	2.15	21	no	−0.9
BaF_2	4.89	1280	2.03	3.10	6.5	30.7	630^s	300^s	1.50	36^s	no	-1.3^s
							0.9^f	220^f		3.4^f		$\sim 0^f$
CsI(Tl)	4.51	621	1.86	3.57	5.6	39.3	1300	560	1.79	165	slight	0.3
CsI(pure)	4.51	621	1.86	3.57	5.6	39.3	35^s	420^s	1.95	3.6^s	slight	−1.3
							6^f	310^f		1.1^f		
$PbWO_4$	8.3	1123	0.89	2.00	10.1	20.7	30^s	425^s	2.20	0.083^s	no	−2.7
							10^f	420^f		0.29^f		
LSO(Ce)	7.40	2050	1.14	2.07	9.6	20.9	40	402	1.82	83	no	−0.2
$LaBr_3$(Ce)	5.29	788	1.88	2.85	6.9	30.4	20	356	1.9	130	yes	0.2

Review of Particle Physics
Journal of Physics G, Vol 37, No 7A (2010)

Light output of NaI(Tl) ~ 40,000 γ/MeV

Crystal Scintillators

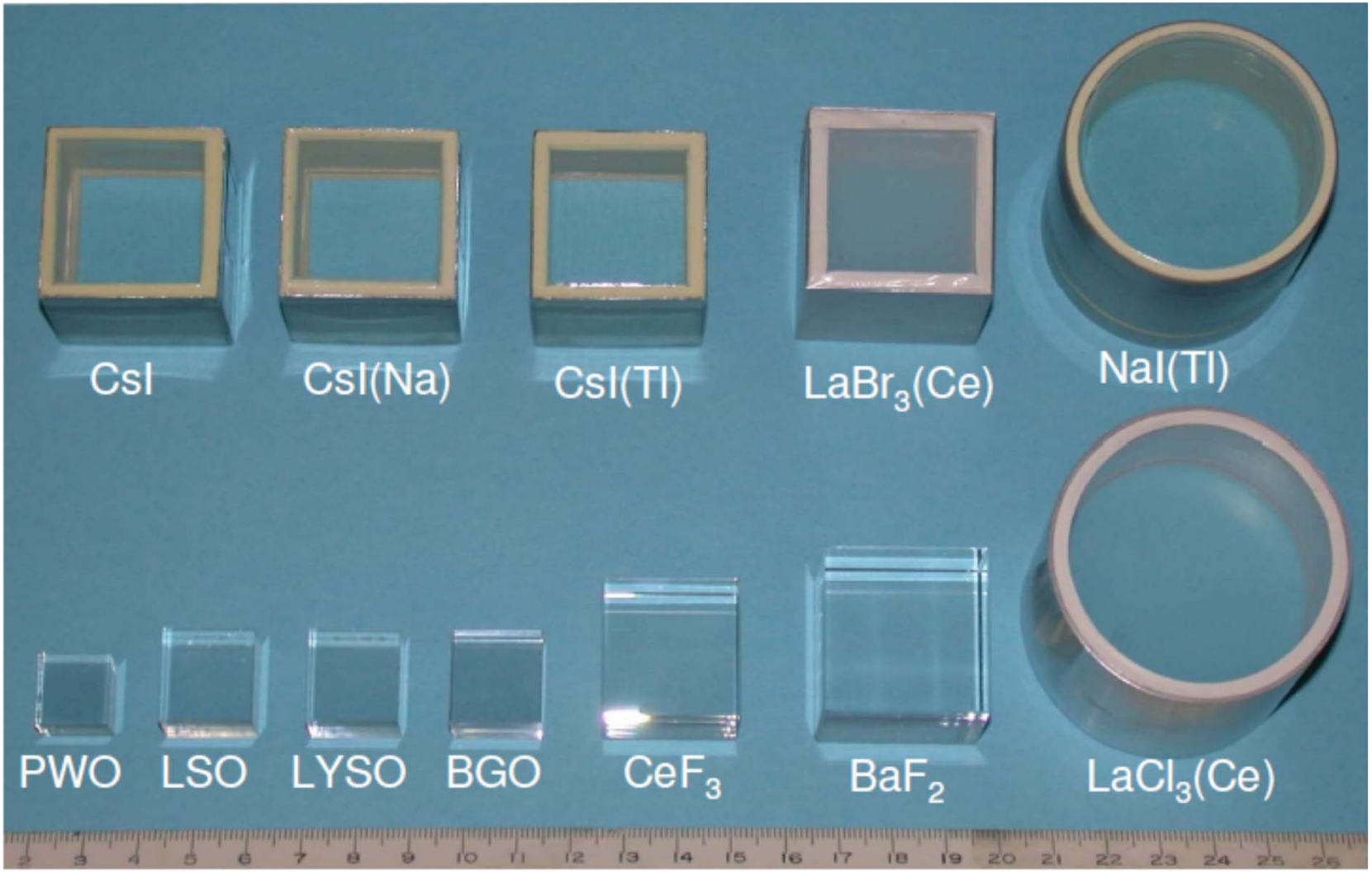

R.Zhu, IEEE Trans. Nucl. Sci., Vol 55, No. 4 (2008) 2425-2431

Crystal scintillators with ~$(1.5\ X_o)^3$ volume

Scintillator Non-Proportionality

Crystal scintillators also do not responds linearly to ionization density

Similar saturation effects occur as in plastic scintillators

Light yield depends on energy and particle type

Can cause significant worsening of energy resolution, particularly at low energies

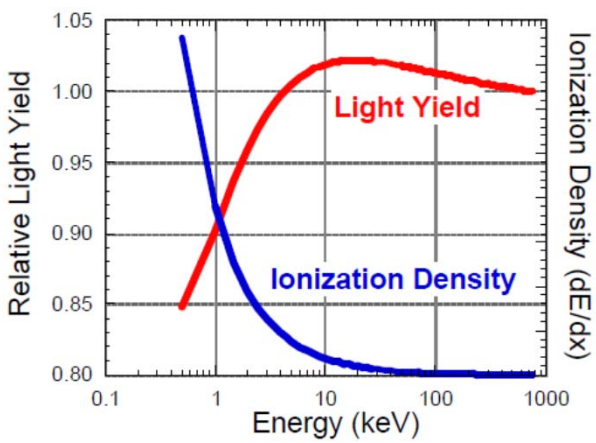

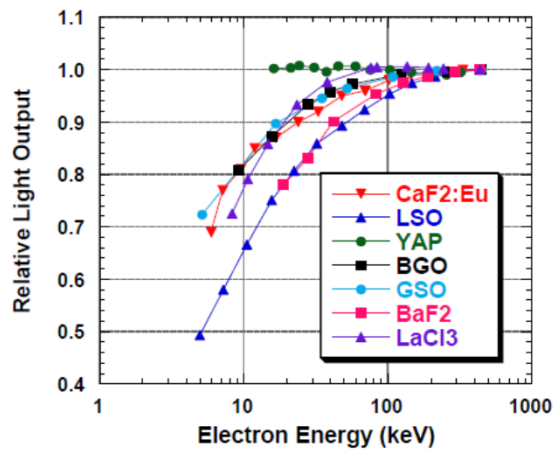

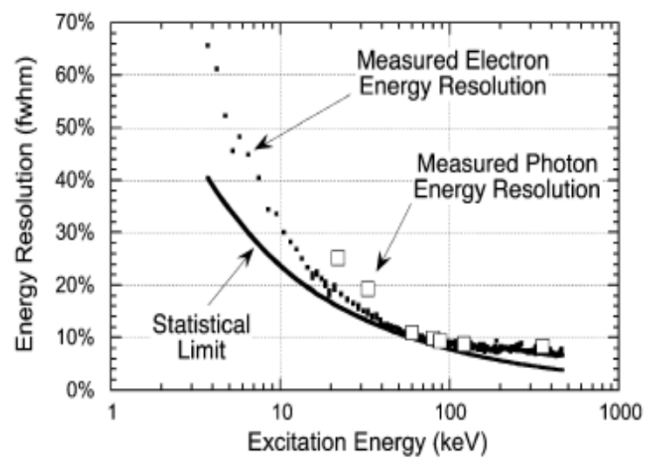

W.Moses, IEEE Trans. Nucl. Sci NS55 (2008) 1049-1053

W.Mengesha et.al., IEEE Trans. Nucl. Sci 45 (1998) 456-461

Cherenkov Radiators

$$\cos\theta_c = \frac{1}{n\beta}$$

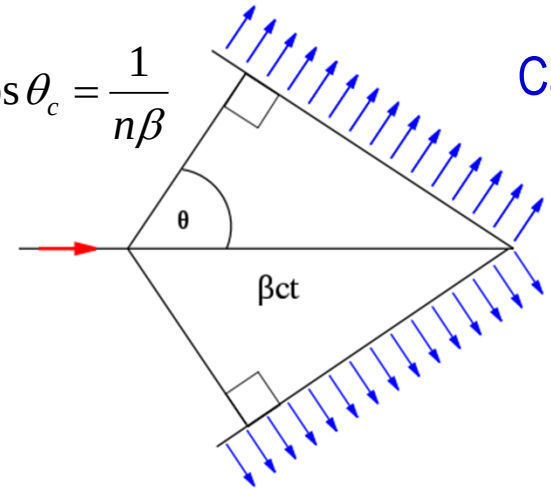

Can be used as threshold detectors or Ring Imaging Detectors

Sensitive to most relativistic particles, so for calorimetry, measures electromagnetic component of shower

	Air	Aerogel	Water	Quartz	PbGl	PbF2
Density (g/cm^3)	1.2x10^{-3}	0.2-0.4	1.00	2.2	6.3	7.77
Index of refraction	1.0003	1.01-1.10	1.33	1.46	1.8	1.78
Radiation Length (cm)	3.1x10^4	68-136	36	12.3	1.26	0.93
N_{pe}/cm for N_0=100	0.06	9	43	53	69	68

$$\frac{dN}{d\lambda} = 2\pi\alpha \sin^2\theta_c \frac{1}{\lambda^2} \quad \Rightarrow$$ Spectrum peaks in the deep (V)UV

$$N_{pe} = L\frac{2\pi\alpha}{hc}\int \varepsilon(E)\sin^2\theta_c(E)dE \qquad \varepsilon = \varepsilon_{col}\cdot\varepsilon_{det}$$

Figure of Merit : $N_0 = 370 cm^{-1} eV^{-1}\int \varepsilon(E)dE$

$$N_{pe} = LN_0\langle\sin^2\theta_c\rangle$$

Timing Measurements

Time resolution determined by:
- Decay time of detector material
- Time response of photodetector
- Light yield of detector material

- Cherenkov materials give fastest time response
- Multichannel plate photodetectors have fastest rise time and smallest transit time spread

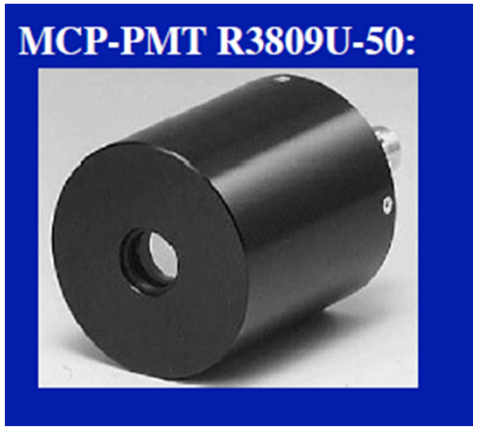

Hamamatsu

6 mm pore diameter
11 mm dia photocathode
~ 10 ps TTS
RT ~ 150 ps
QE ~ 26% at 407 nm
PDE ~ 50-60% relative to PMT

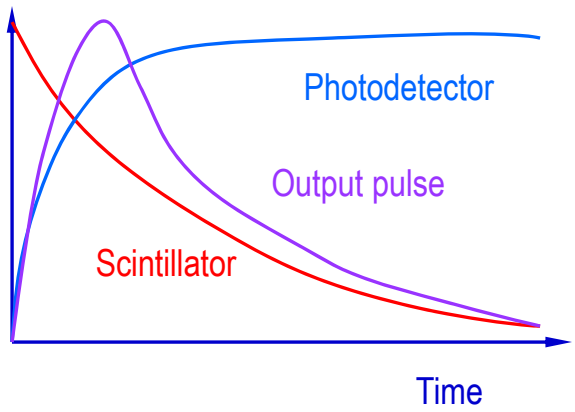

Photoelectron arrival time is a statistical process

If light yield is low, individual photoelectron arrival times will be seen

Best timing achieved by detecting first photoelectron

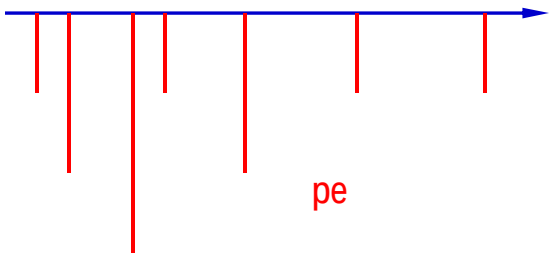

Light Collection

Light produced in the gamma converter must be collected and directed onto the photodetector.

Light collection techniques

- Direct reflection or use of reflective materials
- Light guides
- Wavelength shifters

Factors to consider

- Efficiency
- Uniformity
- Geometry
- Matching to readout device

Reflectors

Diffuse reflection
Lamberts Law

$$\frac{dI(\phi)}{dI_0} = \cos(\phi)$$

Critical angle

$$\theta_c = \sin^{-1}\frac{n_1}{n_0}$$

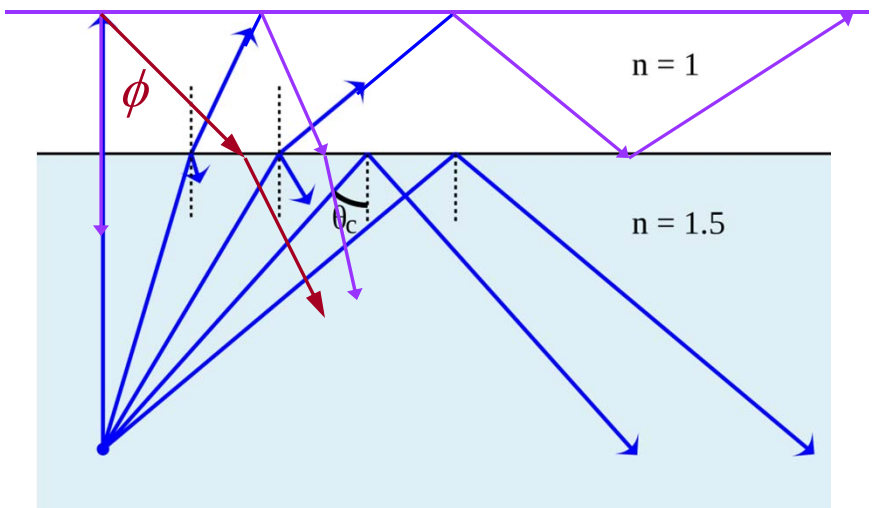

Best reflector is Total Internal Reflection

- Scintillation light is produced isotropically
- Some fraction F will be trapped in the scintillator by internal reflection
  - requires good polished surface
  - however, may lead to non-uniformities due to self absorption
- Escaping fraction can be reflected back into scintillator by an external reflector
  - Requires an air gap between scintillator surface and reflector to preserve internal reflection
  - Specular reflector preserves angle
  - Diffuse reflector can change the angle of exiting rays to improve efficiency

Focusing Light Guides

Need to concentrate the light, but Phase Space density $\rho(q,p)$ remains constant with time

Louisville's Theorem

$$\frac{d\rho}{dt} = \sum_{i=1}^{n}\left(\frac{\partial\rho}{\partial q_i}\dot{q}_i + \frac{\partial\rho}{\partial p_i}\dot{p}_i\right) = 0$$

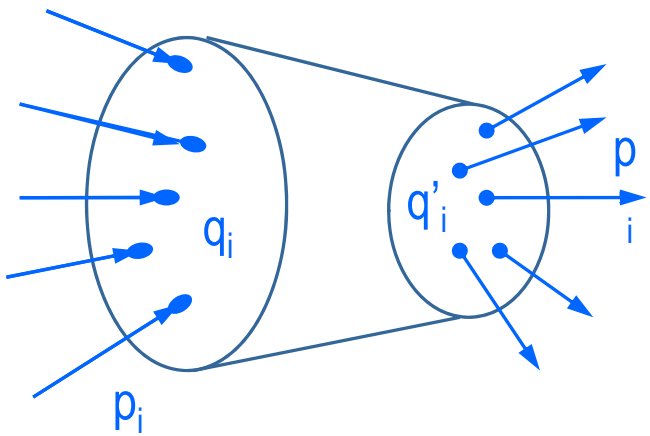

Reducing area increases divergence

Winston Cone

R.Winston, J. Opt. Sci. Amer. 60 (1970) 245-247

Off axis parabola of revolution
Focuses rays on exit aperture

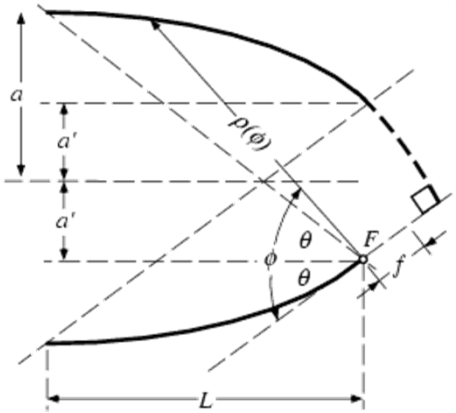

Try to preserve initial area

Adiabatic Light Guide

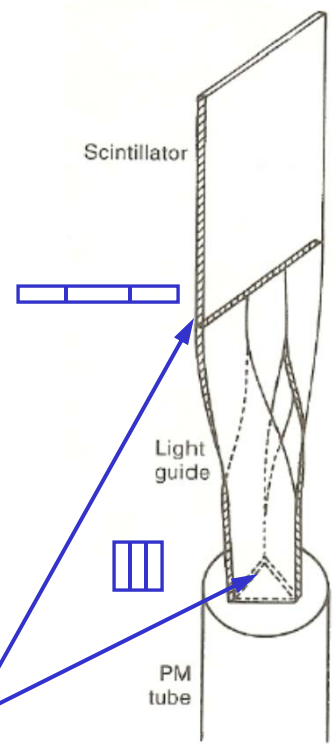

G.Knoll, Radiation Detection and Measurement

Optical Fibers

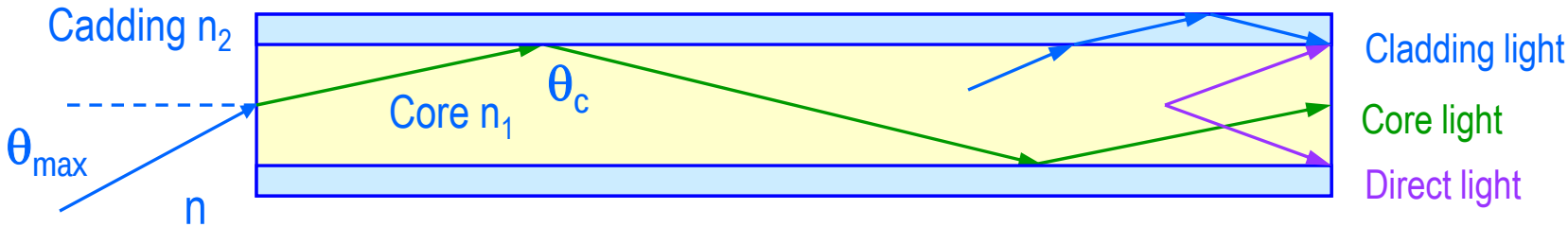

Fibers are used both as light guides and as active detector material
- Scintillator or Cherenkov

Light is trapped by internal reflection between core and cladding ($n_1 > n_2$)

Numerical Aperture defines the maximum angle that can be trapped

$$N.A. = n \cdot \sin\theta_{max} = \sqrt{n_1^2 - n_2^2}$$

Trapping fraction is small

$$F_{fib} = \frac{1}{2}\left(1 - \frac{n_2}{n_1}\right)$$

G.Knoll, Radiation Detection and Measurement

n_1=1.58 (polystyrene)
n_2=1.49 (PMMA)
F_{fib} ~ 3%
x2 ~ 6% if use reflector or read out both ends

Attenuation length is highly wavelength dependent
Some escaping light is trapped in the cladding
Direct light can also escape

All can lead to non-uniformities in Sci-Fi applications

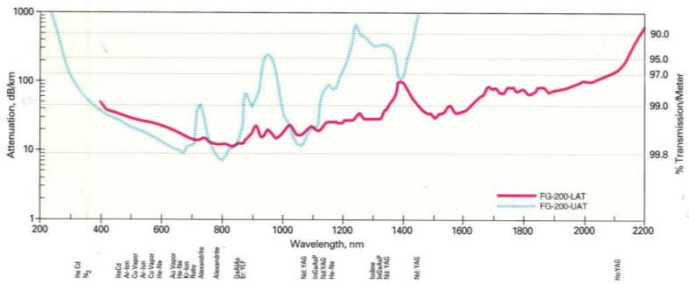

3M Optical Fibers

Wavelength Shifters as Light Collectors

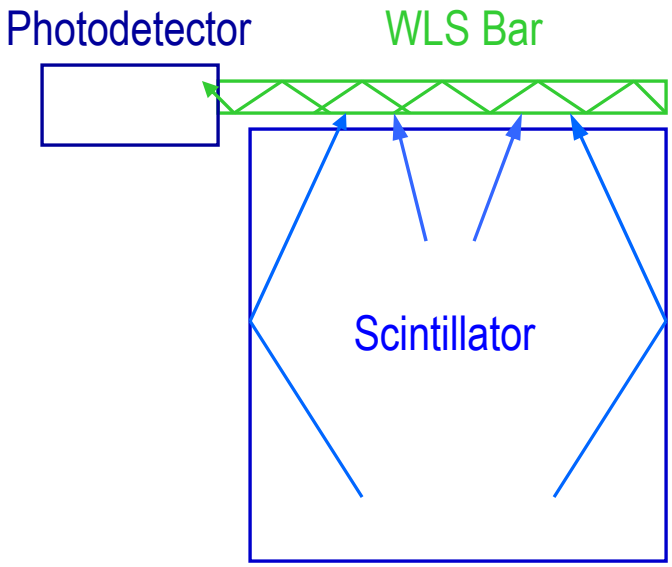

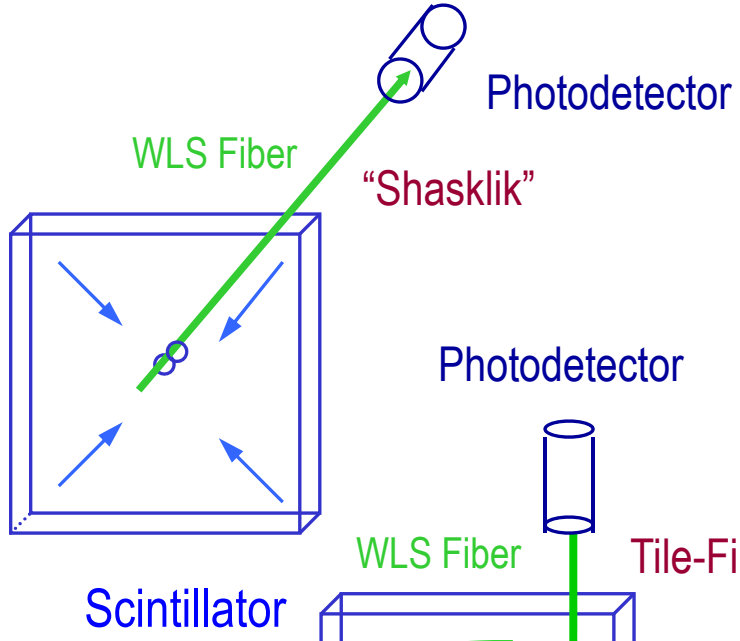

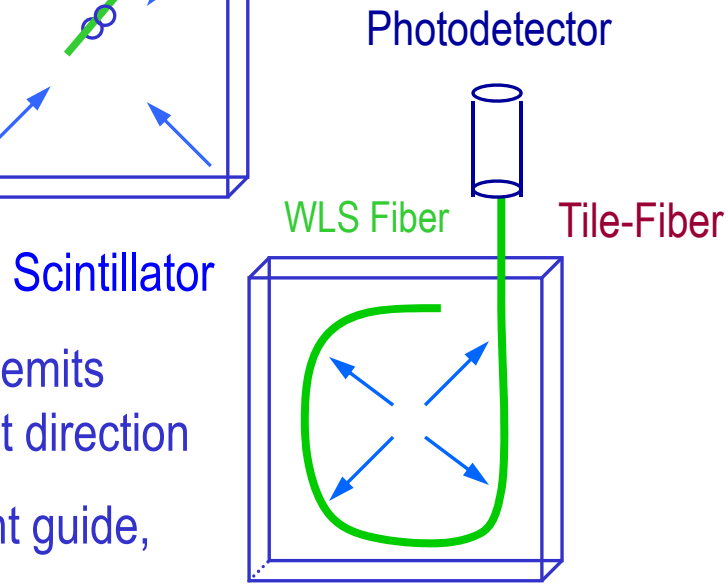

Wavelength shifter absorbs scintillation light and re-emits shifted light at a longer wavelength and in a different direction

Wavelength shifter (bar, fiber,…) acts as its own light guide, bringing the shifted light to the photodetector

Note: Transfer of light from scintillator to wavelength shifter, absorption, re-emission, collection and transfer to photodetector can be very inefficient

Coupling to Photodetector

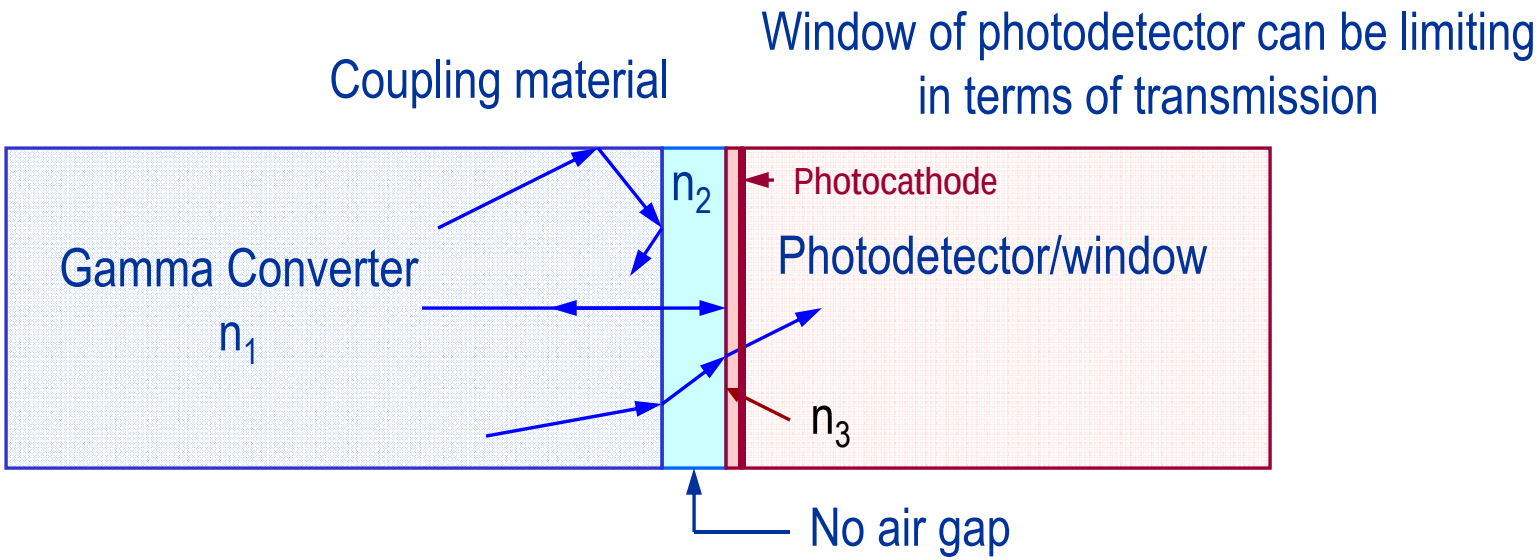

Fresnel loss (normal incidence)

$$R = \left[\frac{n_2 - n_1}{n_2 + n_1}\right]^2$$

n_1=1, n_2=1.5

R ~ 4%

Coupling materials (n~ 1.4):

- Optical grease/glue
- Silicon "cookies"

$\Rightarrow$ n2 ~ n3

However, for heavy crystals $n_1 > n_2$

Examples of Applications of Photodetectors

- Particle Physics
  - Calorimetry
  - Cherenkov Detectors
  - Time of Flight Detectors
- Medical Imaging
  - PET
  - SPECT

Calorimetry

The purpose of calorimetry in particle physics is to measure the total energy of high energy particles.

Energy comes in two forms: electromagnetic and hadronic

Calorimeters come in two types: sampling and homogenous

Requirements for good energy resolution:

- Detect as much as possible of the total energy (best for homogenous)
- Equalize response for electromagnetic and hadronic energy
- High light yield ($\Rightarrow$ good photostatistics)
- Good uniformity (both longitudinally and transverse)

$$\frac{\sigma_E}{E} = \frac{a}{\sqrt{E}} \oplus \frac{b}{E} \oplus c$$

Sampling fluctuations + photostatistics — Noise — Constant

Sampling Calorimetry

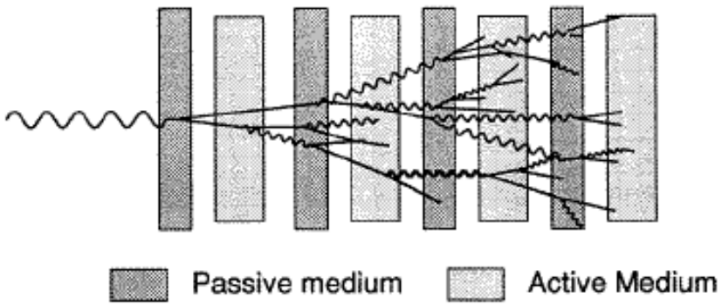

R.Wigmans, Calorimetry Energy Measurement in Particle Physics

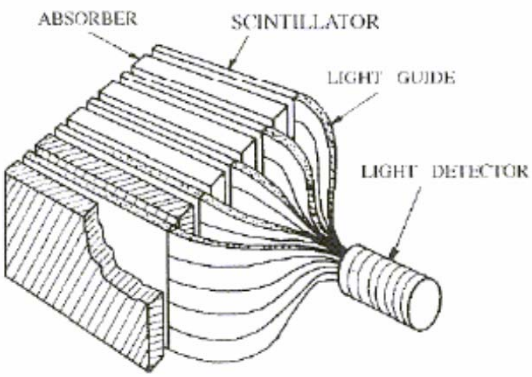

Direct readout

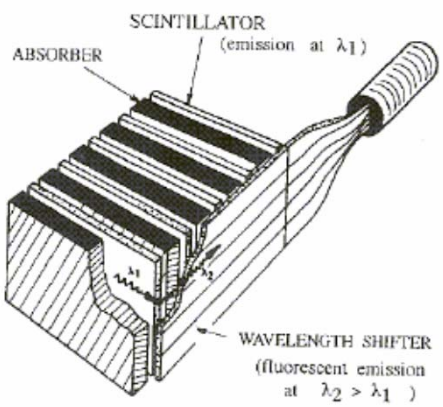

WLS Bar Readout

Alternating layers of passive material (absorber) and active medium to measure the energy of high energy particles

With scintillator as the active medium, problem is to collect the light onto the photodetector

Most direct collection techniques produce unfavorable geometry for stacking modules or creating calorimeters which are hermetic (i.e., without cracks or dead material)

Want good uniformity (longitudinal and transverse) to give good energy resolution

Fiber Calorimeters

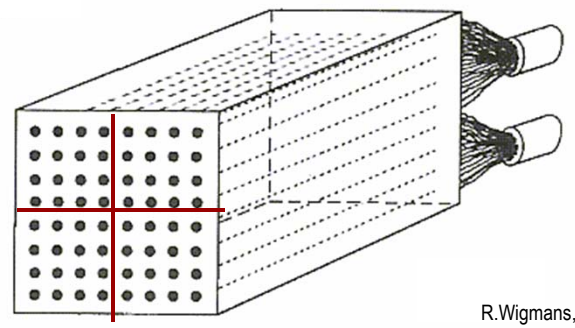

R.Wigmans, Calorimetry Energy Measurement in Particle Physics

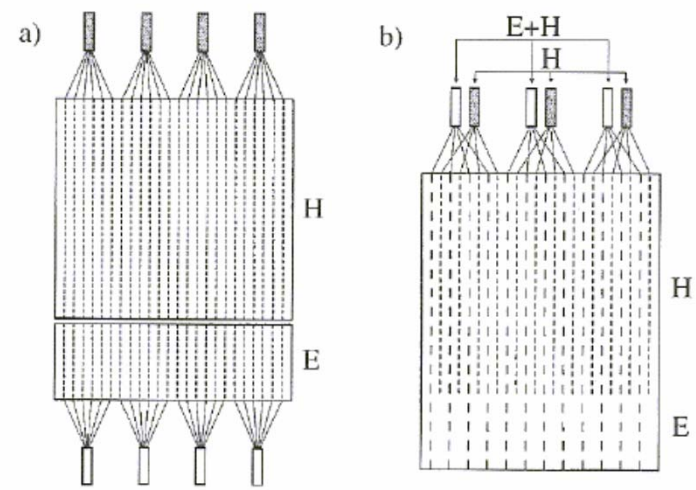

Fibers form the active medium which are interspersed longitudinally with the absorber material

Brings light to the back of the calorimeter where photodetector can be attached

Fibers can be plastic scintillator, wavelength shifter or Cherenkov material, or a combination

Electromagnetic (front) and Hadronic (back) sections can be read out separately using different fibers

Allows almost any degree of transverse segmentation

The SPACAL "Spaghetti" Calorimeter

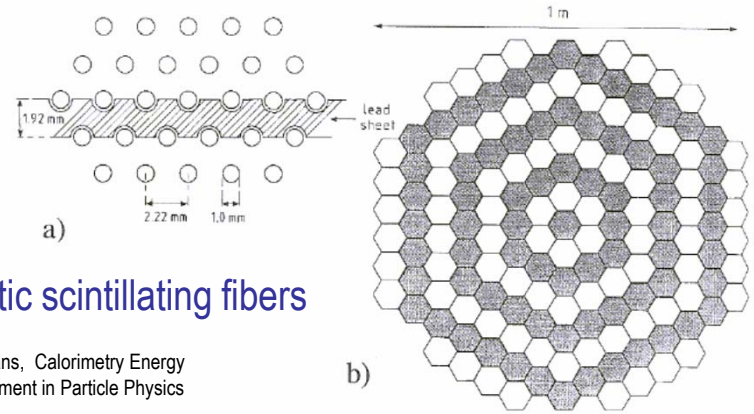

1 mm plastic scintillating fibers

R.Wigmans, Calorimetry Energy Measurement in Particle Physics

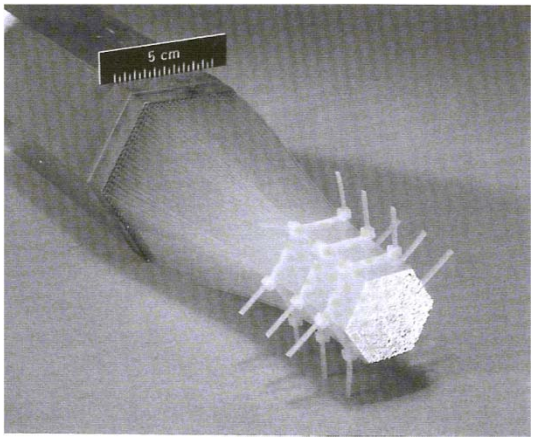

First calorimeter based on scintillating fibers as the active medium
- very compact (80% absorber)
- small sampling fraction (2.3%)
- could be made hermetic with fine segmentation

Fibers brought to back, bundled and read out with 2" PMTs

Photostatistics → 300 p.e./GeV

⇒ ~ 6%/√E contribution to energy resolution

$$\left(\frac{\sigma_E}{E}\right)_{EM} = \frac{13\%}{\sqrt{E}} \oplus 1\% \qquad \left(\frac{\sigma_E}{E}\right)_{Had} = \frac{33\%}{\sqrt{E}} \oplus 2.2\%$$

Other Sci-Fi Calorimeters
H1
KLOE
JETSET
CHORUS
E864 (BNL)

The 'Dream Calorimeter'

DREAM = Dual REAout Module

R.Wigmans
Texas Tech University

Concept:

Measure electromagnetic and hadronic energy separately event by event

Use Cherenkov fibers to measure EM component, plastic fibers to measure hadronic component

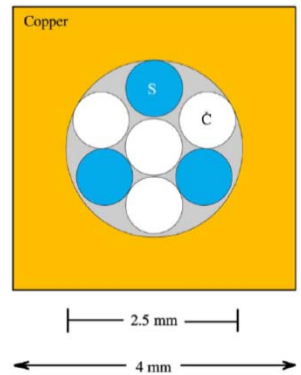

Copper absorber (2 m long)
4 Cherenkov fibers
(quartz + clear plastic)
3 Plastic scintillating fibers

~ 18 p.e./GeV plastic,
~ 8 p.e./GeV quartz

Uncorrected

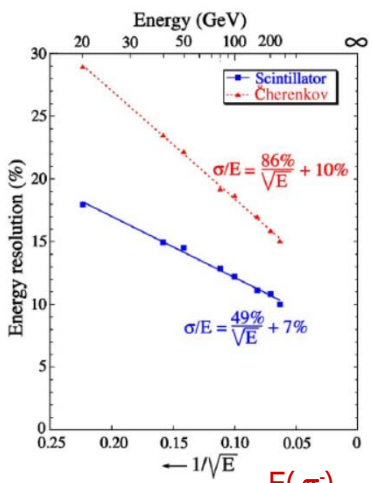

E(π^-)

Quartz-Scintillator correlation
(event-by-event)

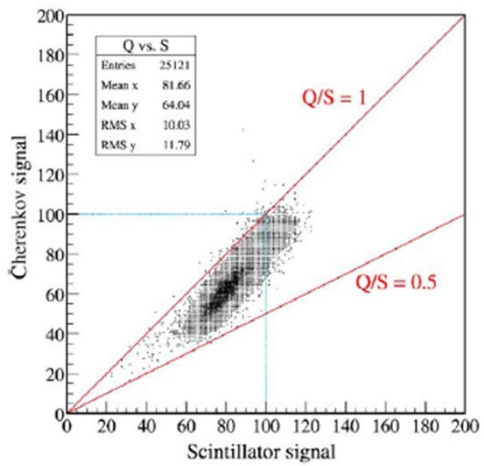

100 GeV π^-

Corrected

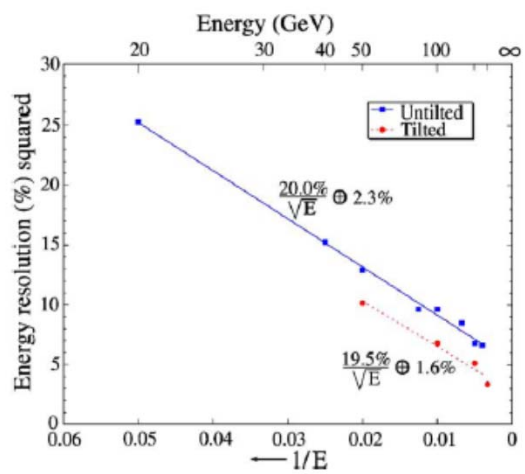

E(π^-)

N.Akchurin et.al., NIM A537 (2005) 537

Dual Readout Using Crystals

BGO Example

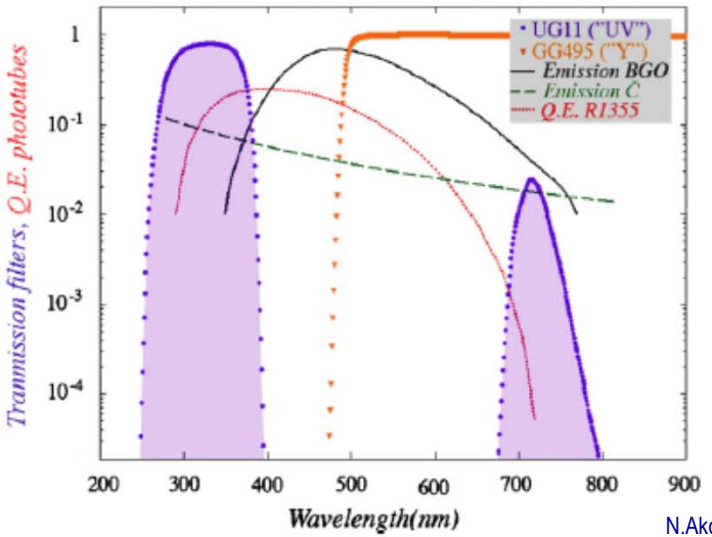

All charged particles produce scintillation light

Highly relativistic particles (EM component of shower) produces additional Cherenkov

Use spectral and time structure differences to separate EM and hadronic components of shower

N.Akchurin et.al., NIM A585 (2008) 395-374

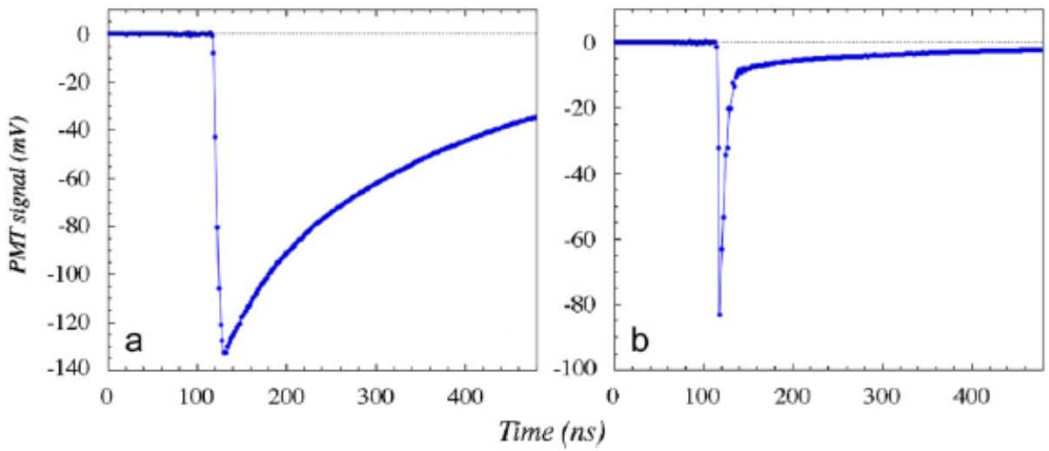

Yellow filter UV filter

Property	Cherenkov	Scintillation
Angular Distribution	Forward peaked cone $\cos\theta=1/n\beta$	Isotropic
Time structure	Instantaneous	few to hundreds of ns
Light spectrum	$1/\lambda^2$	~ 400 nm

Compact Muon Solenoid (CMS)

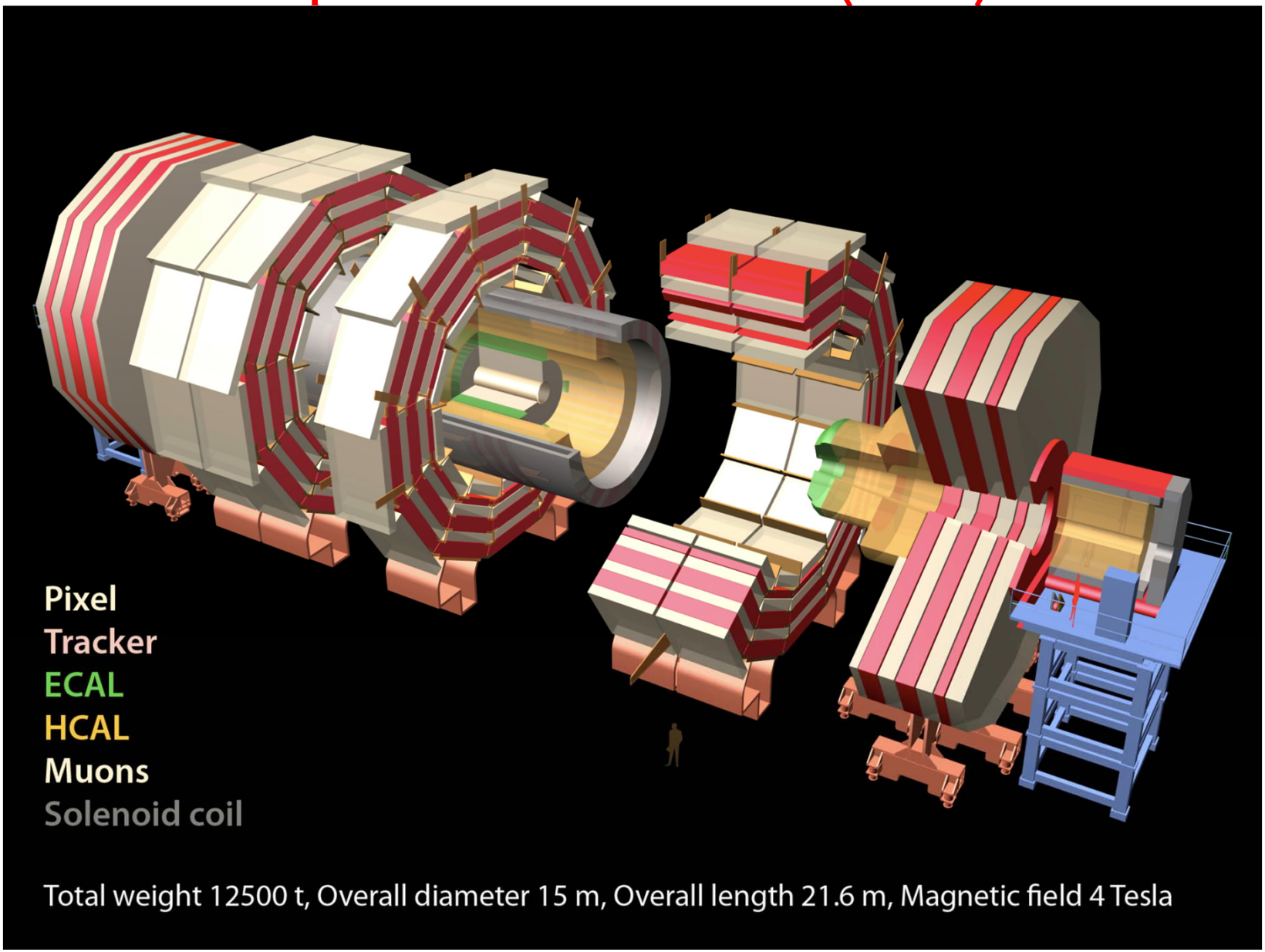

CMS Barrel Hadron Calorimeter

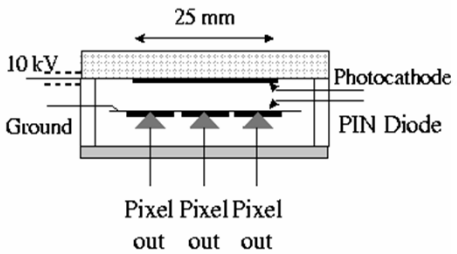

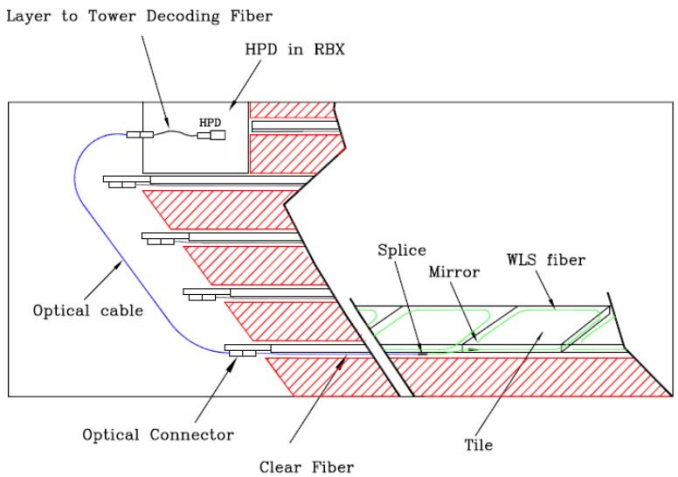

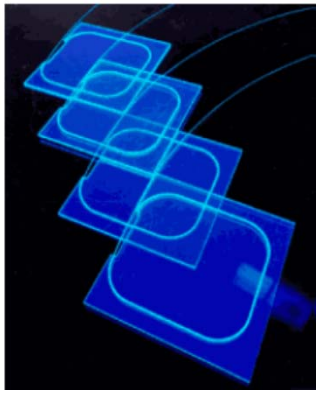

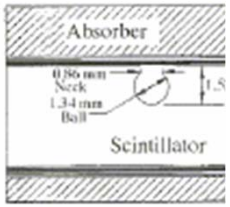

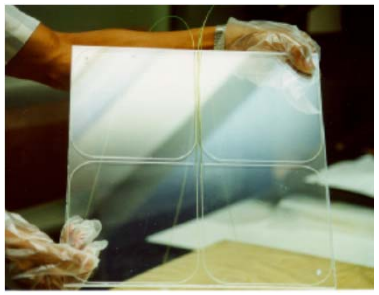

Scintillating tiles read out with WLS fibers placed in groove in the tile

Fibers are read out with Hybrid Photodiodes (HPDs)

- low sensitivity to (axial) magnetic field
- high gain
- low ENF
- large dynamic range

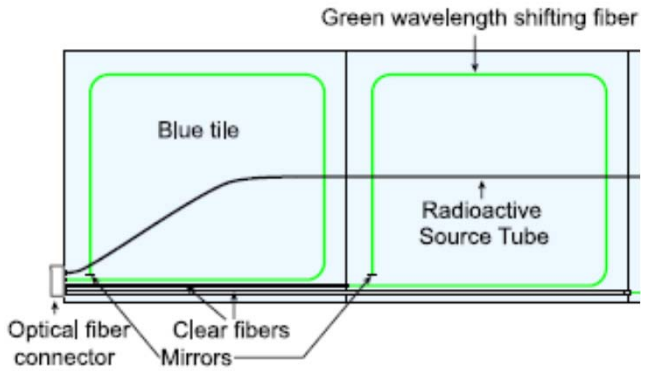

Couple WLS to clear fibers to transport light over long distances (better attn. len.)

Other Tile-WLS Fiber Calorimeters
ATLAS Hadron
LHBb HCAL
STAR EMCAL
D0
HERA
CALICE (w/SiPMs)

CMS Forward Hadron Calorimeter

Quartz fiber calorimeter

- Steel absorber
- 100 km quartz fiber
- PMT readout (quartz window)
- Extremely high radiation levels (~ 100 Mrad/yr)
- Extremely high rates (~ 10^{11}/cm^2/sec)

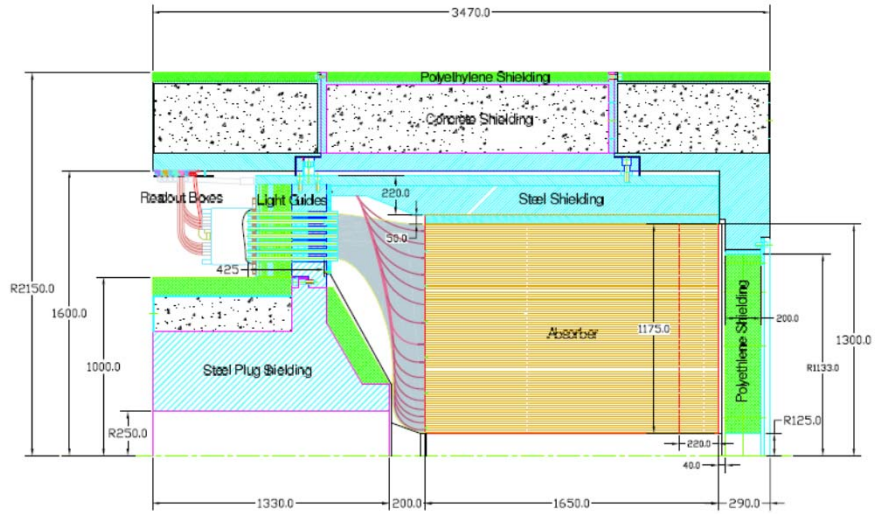

Essentially sensitive only to EM component of shower (Cherenkov light only)

$\Rightarrow$ Poor resolution (dominated by photostatistics) but measures very high energies

$$\left(\frac{\sigma_E}{E}\right)_{EM} = \frac{198\%}{\sqrt{E(GeV)}} \oplus 9\%$$

$$\left(\frac{\sigma_E}{E}\right)_{had} = \frac{280\%}{\sqrt{E(GeV)}} \oplus 11\%$$

CMS Electromagnetic Calorimeter

S.Chatrchyan et.al., JINST Vol.3 (2008) S08004

Barrel: $|\eta| < 1.48$
61200 crystals (2x2x23 cm^3)
Read out with Si APDs

Granularity Barrel
$\Delta\eta x \Delta\varphi = 0.0174 x 0.0174$

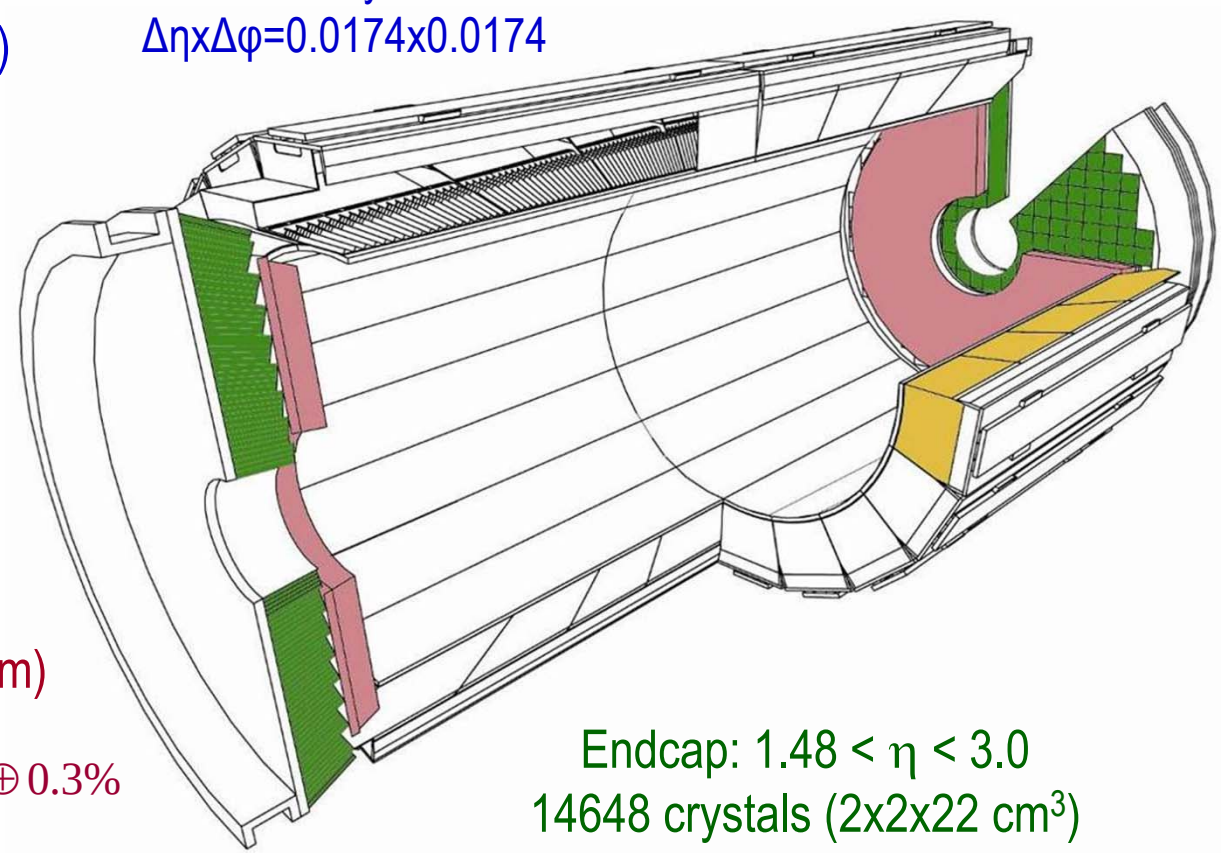

75468 $PbWO_4$ Crystals
X_0 = 0.89 cm
R_M = 2 cm

Barrel Resolution (Test Beam)

$$\frac{\sigma(E)}{E} = \frac{2.8\%}{\sqrt{E(GeV)}} \oplus \frac{125MeV}{E(MeV)} \oplus 0.3\%$$

Endcap: $1.48 < \eta < 3.0$
14648 crystals (2x2x22 cm^3)
Read out with vacuum phototriodes

Lead Tungstate Crystals

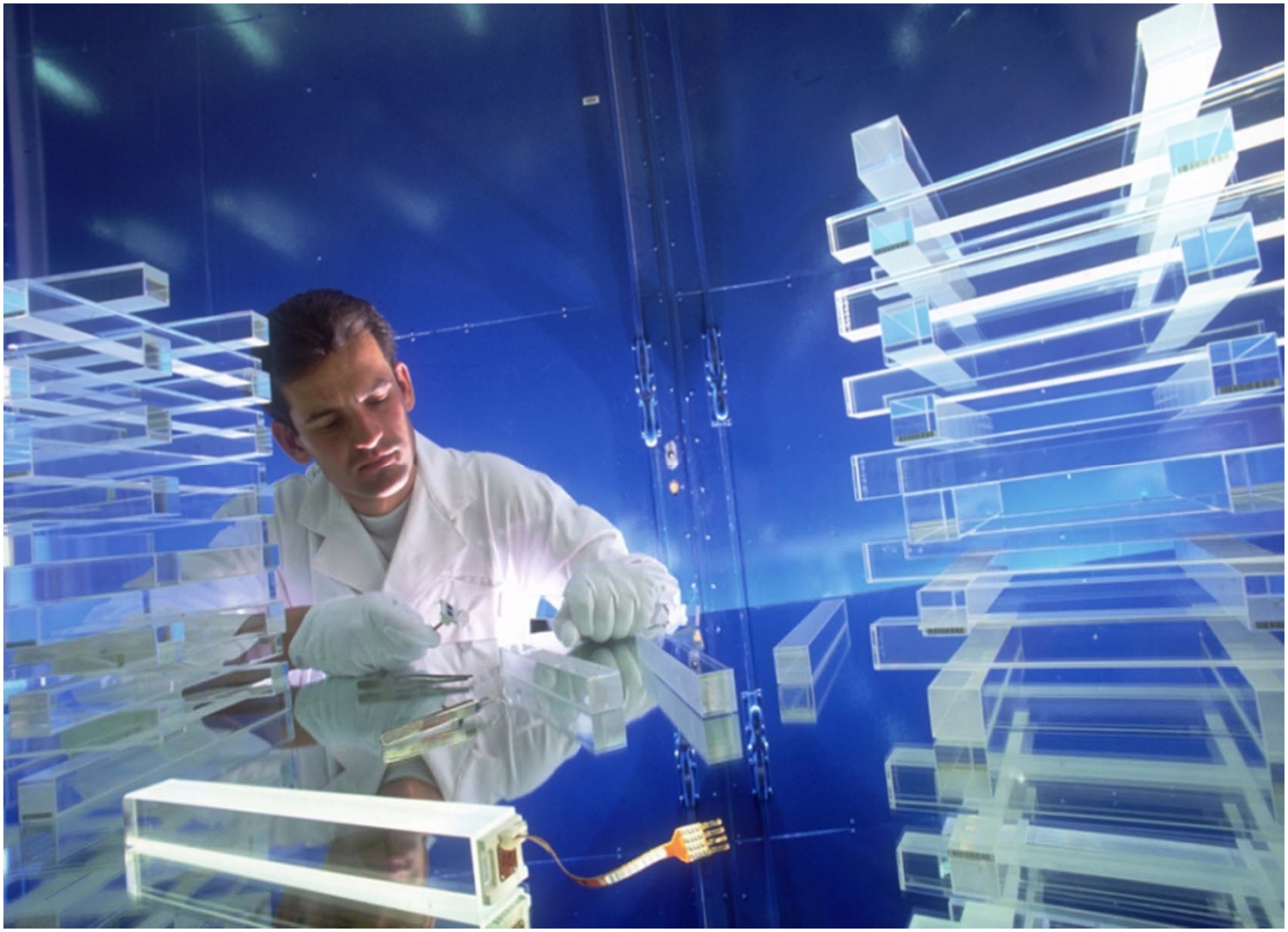

Crystals produced in Russia and China

CMS Barrel EMCAL

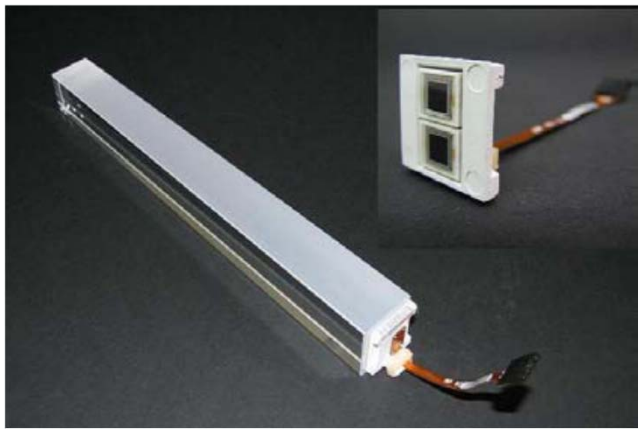

Dual APDs
for redundency
covering ~ 10% of area
~ 4.5 p.e/MeV

Light Yield ~ 100 γ/MeV
Uniformity ~ 0.3%
$|dLY/X_0| < 0.35\%/X_0$
between 3 and 13 X_0

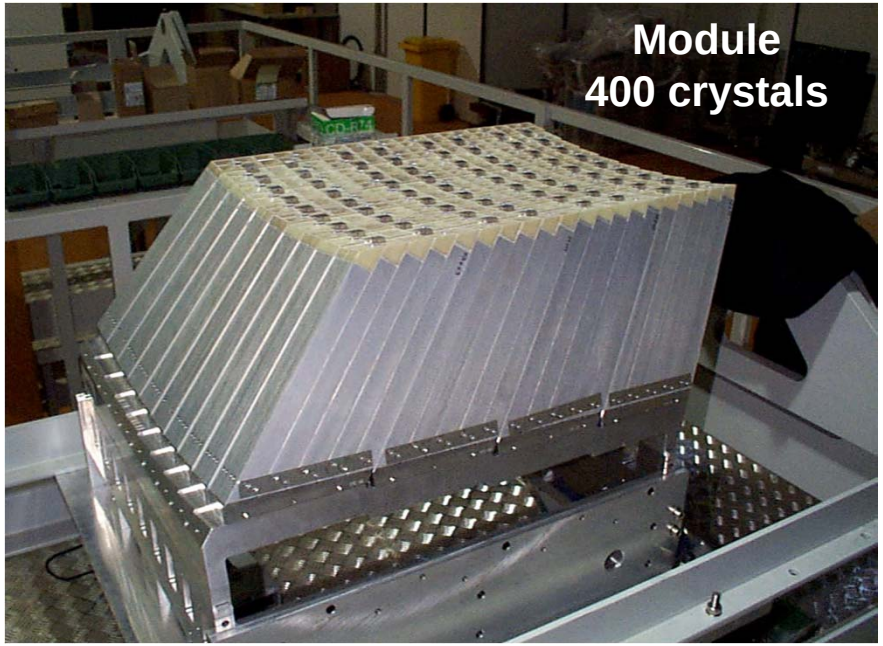

$PbWO_4$ crystals

- Must be extremely uniform to obtain design energy resolution
- Must be radiation hard (achieved after extensive R&D program)

Hammamastu S-8148 (5x5 mm^2)

- Insensitive to magnetic field
- Gain: M=50
- dM/dV = 3%/V, dM/dT = -2.3%/°C
  - requires good V and T stability (~.05°C)
- <Q.E.> ~ 70% with $PbWO_4$
- Nuclear counter effect (minimized depletion layer)

CMS Endcap EMCAL

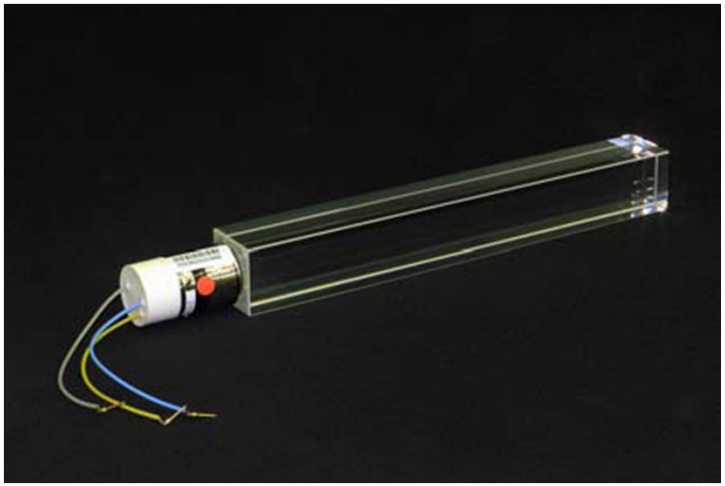

~ 4.5 p.e/MeV

(larger area
lower QE
than APDs)

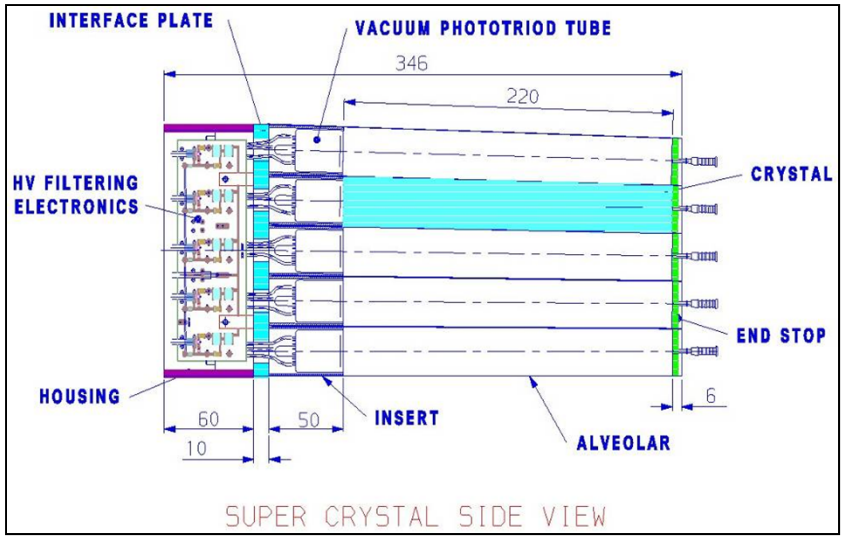

Vacuum Phototriode (Research Institute Electron, St. Petersburg, Russia)

- Single gain stage PMT (1" dia)
- <QE> ~ 22% at 420 nm
- Minimal sensitive to magnetic fields (15% loss at 4T)
- Gain: M=10
- Quartz window
- Rad tolerance < 10% after 20 KGy (could not use APDs due to higher radiation levels)

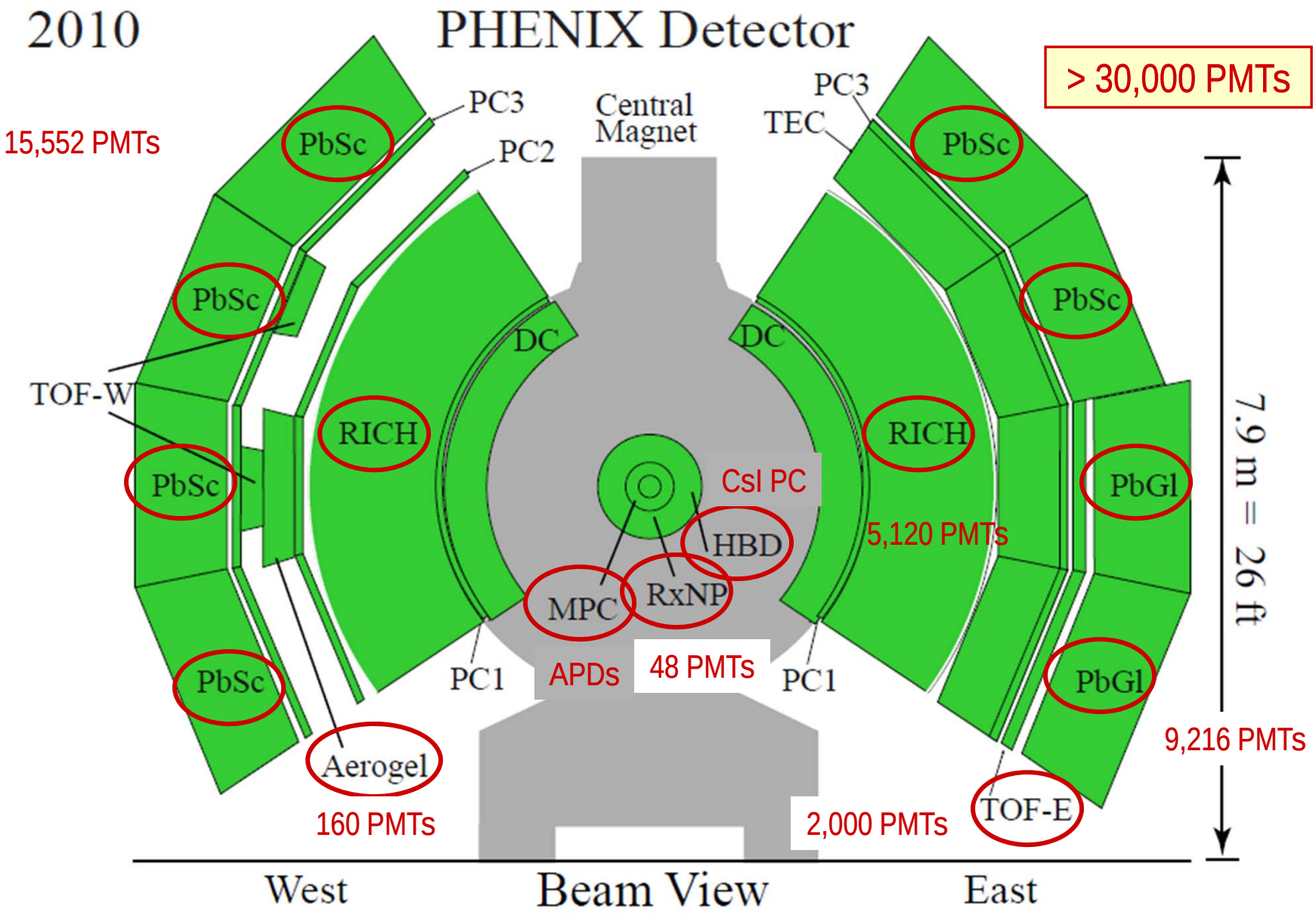
2010
PHENIX Detector
> 30,000 PMTs
15,552 PMTs
PbSc
PC3
PC2
Central Magnet
TEC
PC3
PbSc
PbSc
PbSc
DC
DC
TOF-W
RICH
RICH
PbSc
PbGl
CsI PC
HBD
5,120 PMTs
MPC
RxNP
PC1
APDs
48 PMTs
PC1
PbSc
PbGl
7.9 m = 26 ft
9,216 PMTs
Aerogel
160 PMTs
2,000 PMTs
TOF-E
West
Beam View
East

PHENIX "Shashlik" EM Calorimeter

"Shashlik" = "Shish-Kebab"

Fine segmentation for high multiplicity heavy ion collisions
$\Delta\eta$ =0.01, $\Delta\phi$ = 0.01 $\Rightarrow$ 5.5 x 5.5 cm^2 "towers" at R=5m
15,522 towers total

Alternating stack of lead and scintillator plates
Wavelength shifting fibers pass longitudinally through the stack
Fibers are bundled in the back and read out with PMTs

Other Shashlik Calorimeters
LHCb EMCAL
ALICE EMCAL
HERA-B

Pb (1.5 mm) Scint (4 mm) 66 layers (18 X_0)

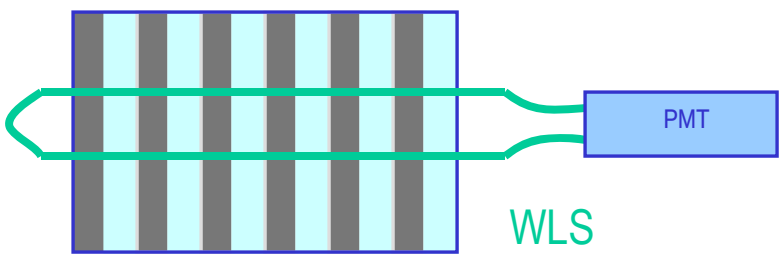

Light Yield ~ 1.5 p.e./MeV

$$\frac{\sigma_E}{E} = \frac{8.1\%}{\sqrt{E}} \oplus 2.1\%$$

$$\sigma_t \sim 200\,ps$$

L.Aphecetche et.al., Nucl. Inst Meth. A499 (2003) 521-526

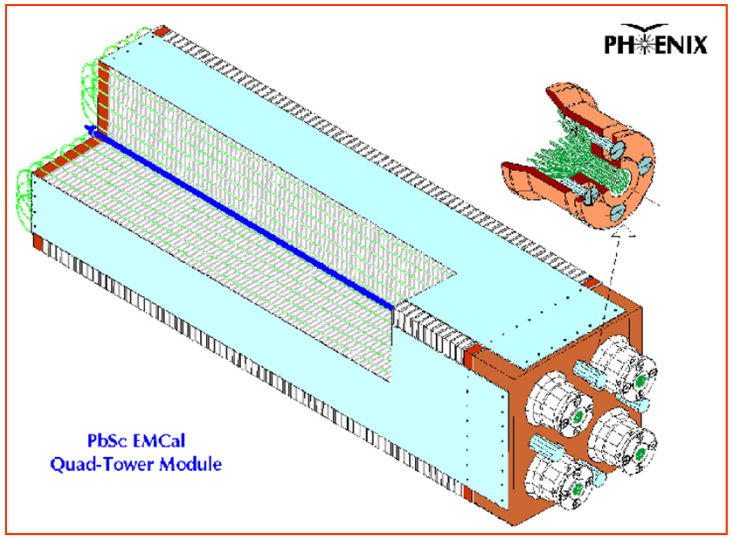

PHENIX PbGl EM Calorimeter

Lead glass acts as a Cherenkov radiator and absorber
Sensitive only to EM component of shower

TF1 lead glass (ρ= 3.85 g/cm^3, n=1.648)
9216 blocks
4x4x40 cm^3 (14.4 X_0)

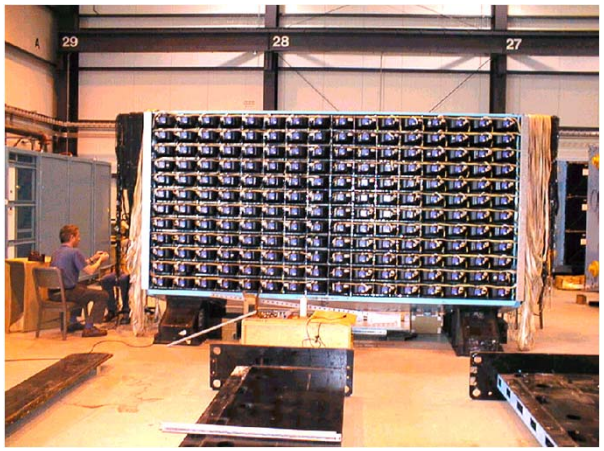

Light Yield ~ 0.5 p.e./MeV

$$\frac{\sigma_E}{E} \sim \frac{5.9\%}{\sqrt{E}} \oplus 0.8\% \quad \sigma_t = 300\,ps$$

Dominated by photostatistics
(no sampling fluctuations)
but note much poorer resolution than crystals

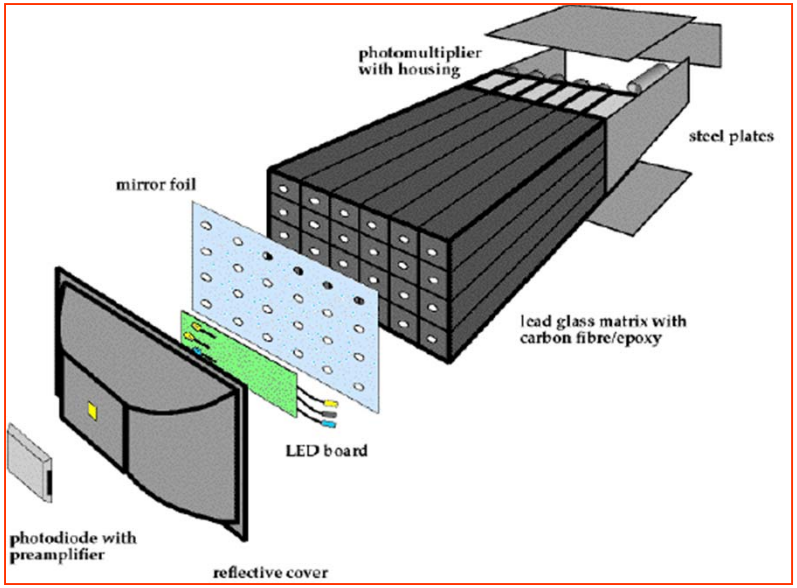

L.Aphecetche et.al., Nucl. Inst Meth. A499 (2003) 521-526

Medical Imaging Applications (mainly PET)

Photodetectors for PET

Ring of Photon Detectors

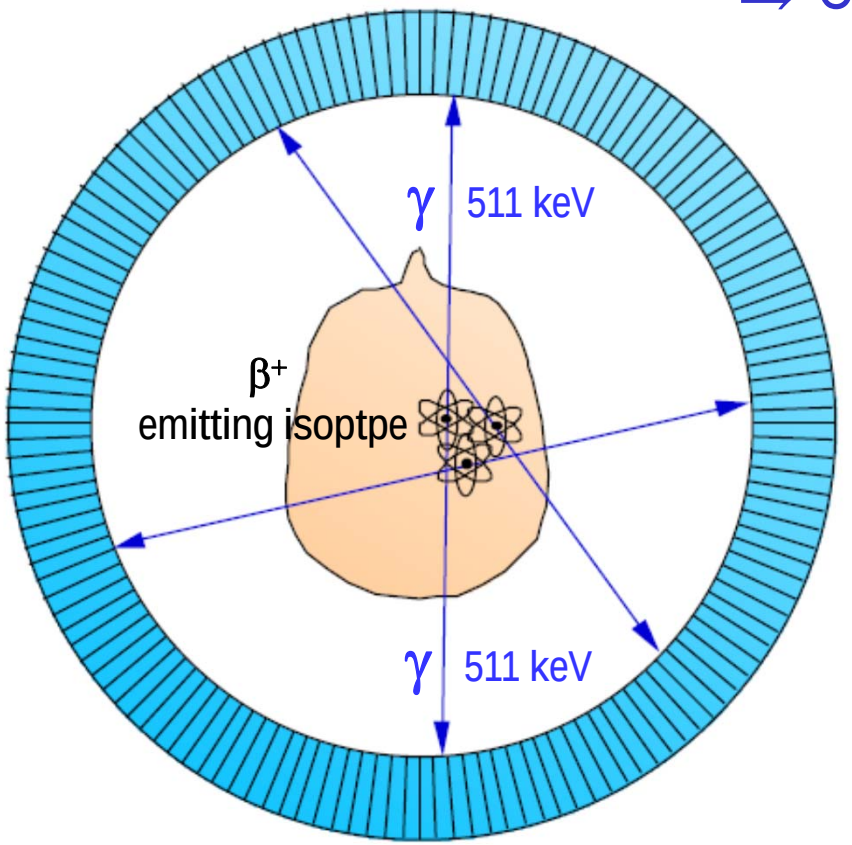

Figure courtesy of W.Moses

511 keV photons require high stopping power

⇒ Crystals such as BGO, LSO, LYSO
(ρ ~ 7 g/cm^3, μ^{-1} ~ 1.2 cm)

Estimate N_{pe}:

Light output: BGO ~ 8400 γ/MeV
LSO ~ 30,000 γ/MeV

- 0.511 MeV
- Light collection efficiency ~ 0.8
- QE

<QE>	PMT	APD
BGO	8.0%	82%
LSO	13.6%	75%

N_{pe}

<Npe>	PMT	APD
BGO	275	2816
LSO	1668	9198

Standard PET Detector

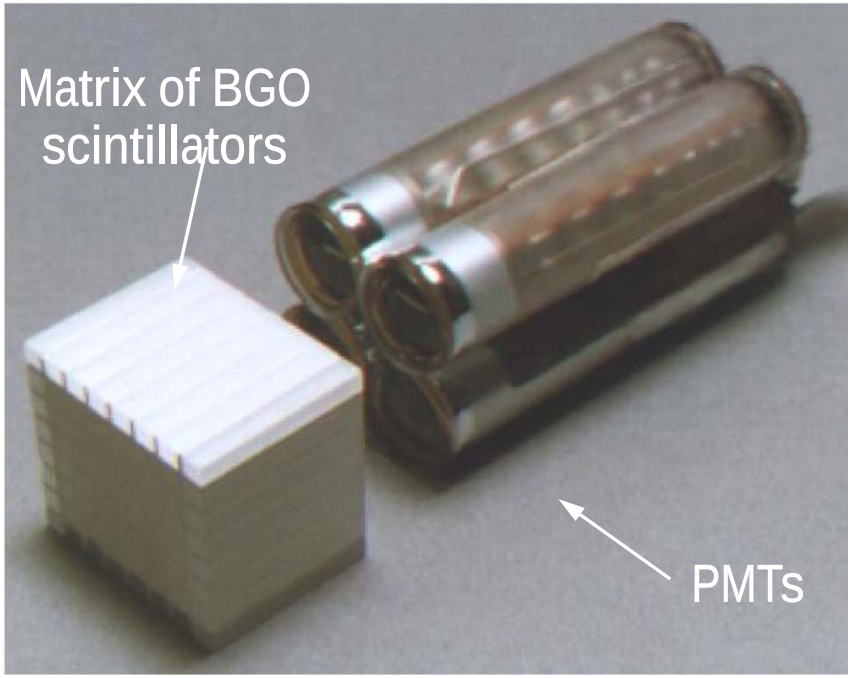

Figures courtesy of M.Casey (Siemens, formerly CTI)

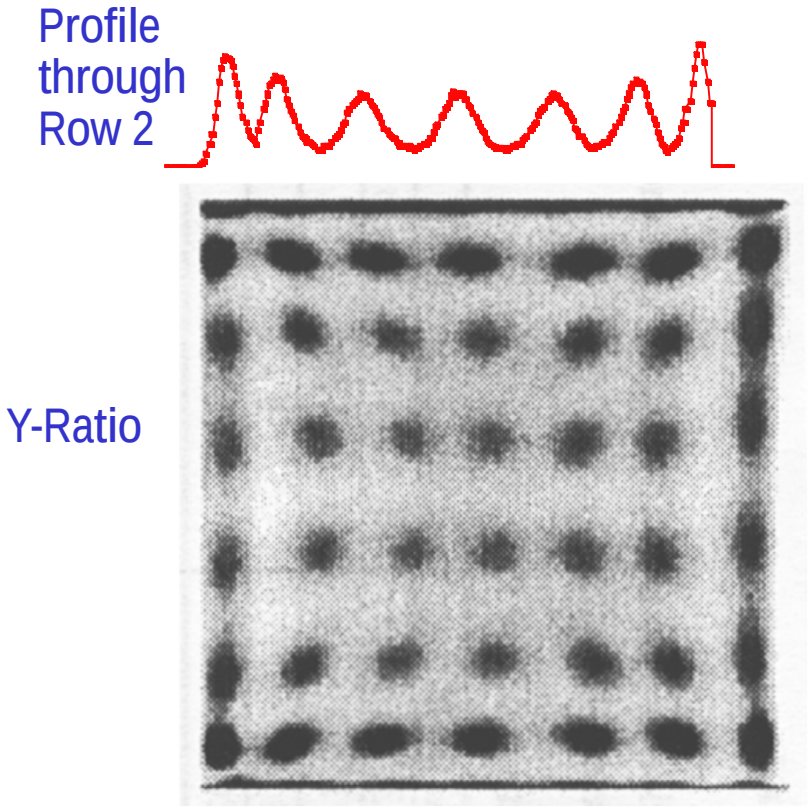

PMTs and BGO have been the workhorse for PET
- used in most clinical human PET scanners
- new scanners are utilizing LSO/YLSO instead of BGO

Position decoded by Anger Logic

Spatial resolution: ~ 4 mm for human scanners
~ 2 mm for small animal scanners

Image is "blurred" due to decoding of which pixel was hit

Spatial Resolution in PET

$$FWHM = 1.25\sqrt{(d/2)^2 + b^2 + (0.0022D)^2 + r^2 + h^2}$$

Geometric Decoding Non-colinearity Positron range DOI

1.25 : degradation due to tomographic reconstruction
d : crystal size
b : uncertainty due to determining block position
D : coincident detector separation
r : effective source size (including positron range)
h : uncertainty in depth of interaction

* Derenzo & Moses, "Critical instrumentation issues for resolution <2mm, high sensitivity brain PET", in *Quantification of Brain Function, Tracer Kinetics & Image Analysis in Brain PET*, ed. Uemura et al, Elsevier, 1993, pp. 25-40.

Contributions to Resolution

Geometrical:

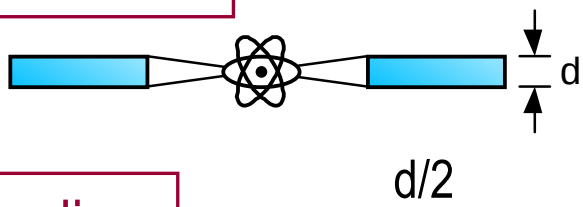

Non-coplanarity:

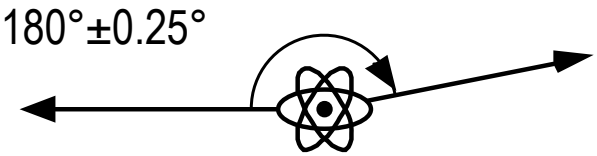

.0044R R=radius of detector

Decoding:

~ 2 mm for standard block detectors
0 mm for 1-1 coupling

Depth of Interaction:

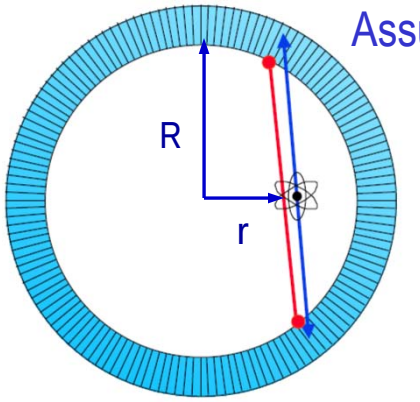

Assuming 30 mm crystals

$$h = 12.5 \frac{r}{\sqrt{r^2 + R^2}}$$

Positron range:

In tissue

Isotope	E_{max} β^+ (MeV)	Effective FWHM (mm)
^{18}F	0.64	0.55
^{11}C	0.96	1.0
^{14}N	1.20	1.4
^{15}O	1.70	2.4

W.Moses & S.Derenzo

How Well Can One Do ?

Assumptions:

- 1-1 coupling
- ^{18}F (shortest range)
- 30 mm thickness
- 10 cm radial FOV

Center of FOV, as a function of crystal width:

Crystal Width (mm)	1.0	0.5	0.0
Decoding (1-to-1coupling)	0	0	0
Range (^{18}F)	0.55	0.55	0.55
Acollinearity (R=100 mm)	0.44	0.44	0.44
Distance from Center (mm)	0	0	0
DOI (30 mm detector thickness)	0	0	0
Reconstruction	1.25	1.25	1.25
Total (mm)	**1.08**	**0.93**	**0.88**

1 mm crystal width, as a function of distance off axis

Crystal Width (mm)	1.0	1.0	1.0	1.0
Decoding (1-to-1coupling)	0	0	0	0
Range (^{18}F)	0.55	0.55	0.55	0.55
Acollinearity (R=100 mm)	0.44	0.44	0.44	0.44
Distance from Center (mm)	0	10	20	30
DOI (30 mm detector thickness)	0	1.24	2.45	3.59
Reconstruction	1.25	1.25	1.25	1.25
Total (mm)	**1.08**	**1.89**	**3.25**	**4.62**

W.Moses & S.Derenzo

Time of Flight PET

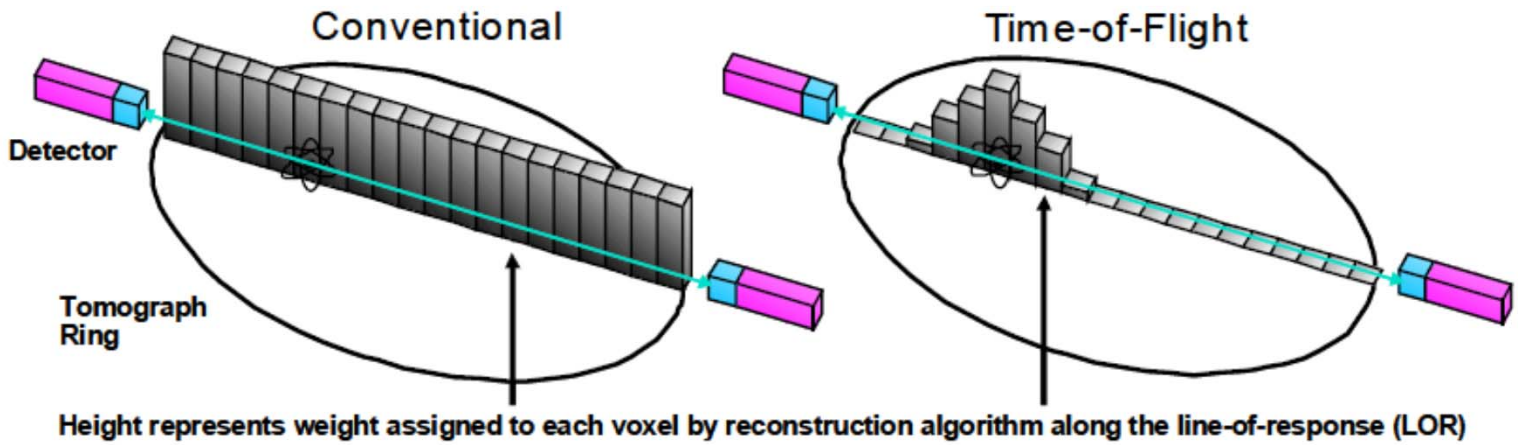

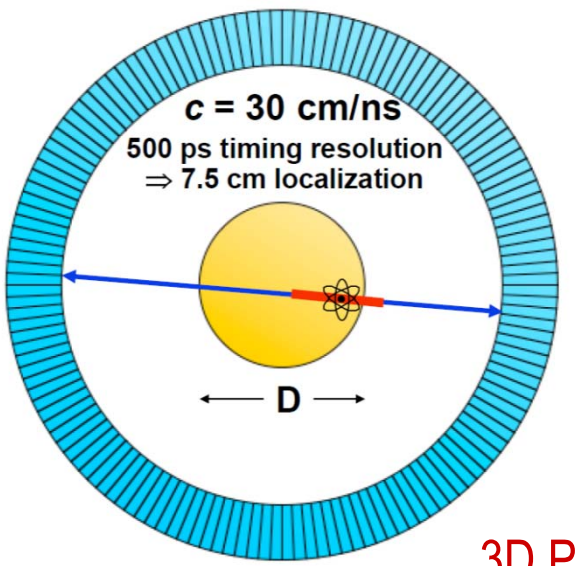

Large randoms background in PET

Use timing information to localize decay point along line

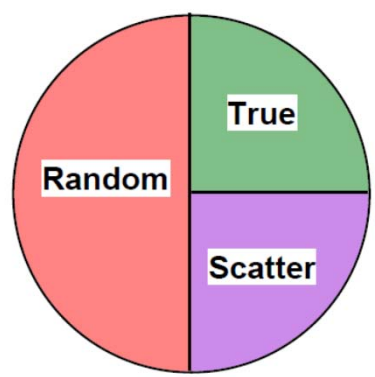

Reduces noise in image

Variance reduction ~ $2D/c\Delta t$

Δt 500 ps $\Rightarrow$ x5 reduction in variance

3D PET

Figures courtesy of W.Moses

Photodetectors for PET

- PMTs
  - Workhorse (not going away any time soon…)
  - Best for timing
  - Bulky, don't stack well (partially solved with multianode PMTs)
  - Don't work in magnetic fields
- APDs
  - Provide sufficient gain for PET applications
  - Work in magnetic fields
  - Strong temperature dependence
  - Not the best for timing (~ few ns)
- SiPMs
  - Provide high gain like PMTs
  - Good time resolution (~ 1 ns or less)
  - Work in magnetic fields
  - Poor packing fraction, but improving with new arrays
  - Strong dependence on bias voltage (operate just slightly above breakdown)
  - High single photoelectron noise

LabPET™

First APD based full size small animal PET scanner

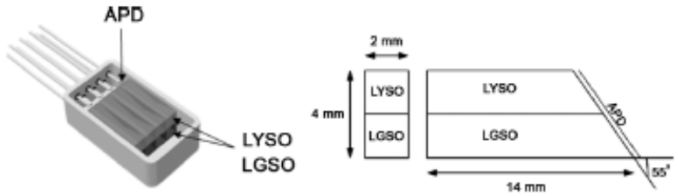

2x2x12/14 mm^3 LYSO(τ~40 ns)/LGSO(τ~60 5ns) crystals in phoswich arrangement

One to one coupling of pixels to APDs

Fully digital electronic readout

Use pulse shape discrimination (in realtime) to determine which crystal was hit

7-9 ns time resolution
2.1 mm spatial resolution
(central 4 cm FOV)

Developed by University of Sherbrooke
and commercialized through AMI-Gamma Medica

LabPET12

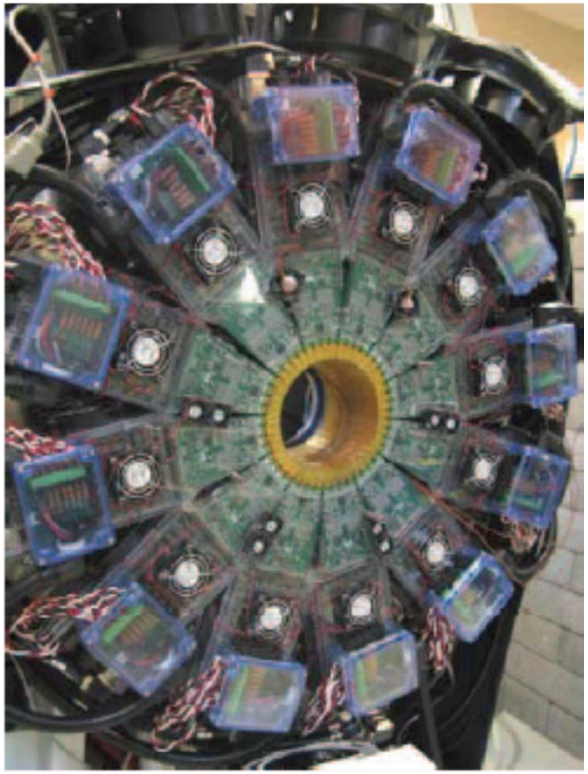

FOV: 16.2 cm dia, 11.25 cm axial

M.Bergdon et.al., IEEE Trans. Nucl. Sci. NS56 (2009) 10-16.
M.-A. Tetrault et.al., IEEE Trans. Nucl. Sci NS55 (2008) 2546-2550

RatCAP

Miniature 3D tomograph designed to image the brain of an awake rat

Compact, ligtweight (<200 g), low power
Can be mounted to the head of an awake rat
40 mm dia x 18 mm axial FOV
12 4x8 array detector blocks
2x2x(5-8) mm LSO direct coupled to matching APD
Custom designed ASIC to provide digital readout
~ 2 mm position resolution
Coincidence time resolution ~ 7 ns

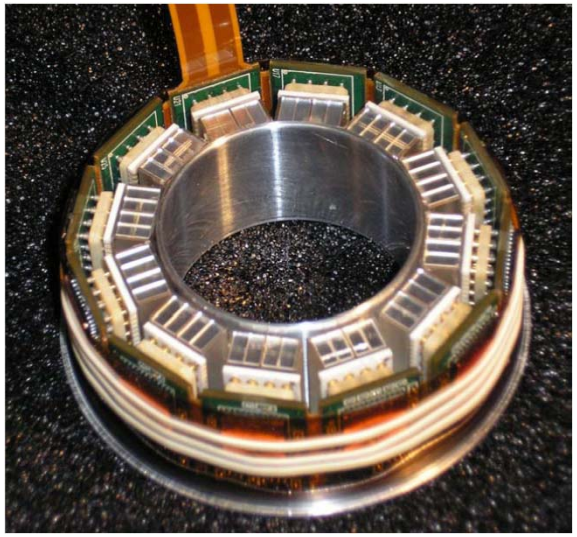

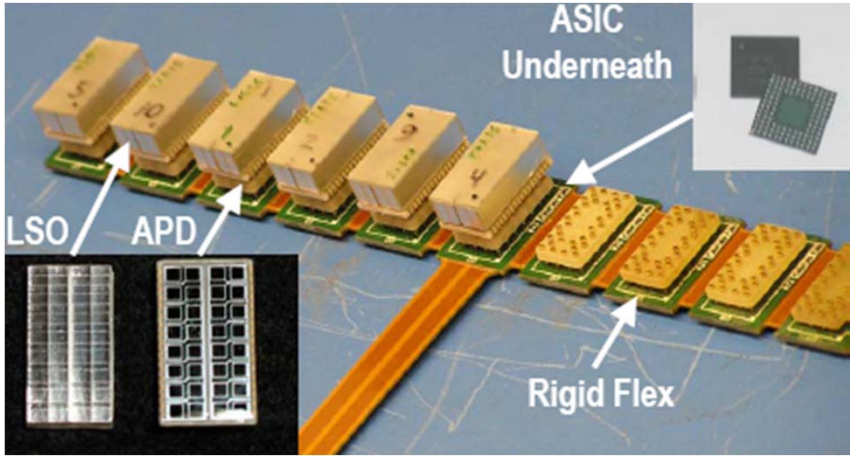

Hamamatsu S8550 APD

P.Vaska et.al., IEEE Trans. Nucl. Sci Vol 51 (2004) 2718-2722

Future trends

Higher spatial resolution, better time resolution for TOF

- Smaller pixel size crystals (<1 mm)
- Fast, high gain photodetector (SiPMs)
- DoI information (continuous crystals)
- Brighter crystals ($LaBr_3$)

0.5 mm^2 LSO matrix

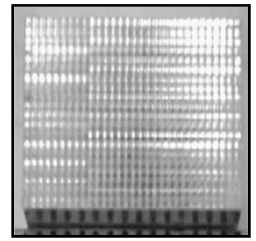

J.Stickel et.al., JNM 48 (2007) 115-121

$LaBr_3$

σ_t < 100 ps

σ_E < 4% @ 511 keV

Direct Coupling of Small Pixels to SiPM Array

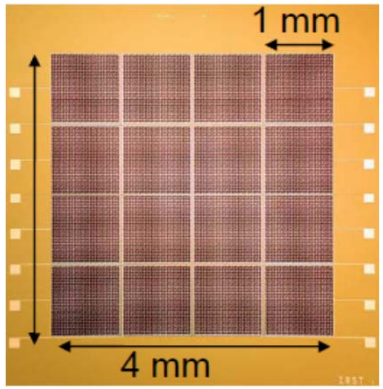

FBK 4x4 array of 1x1 mm^2 SiPMs

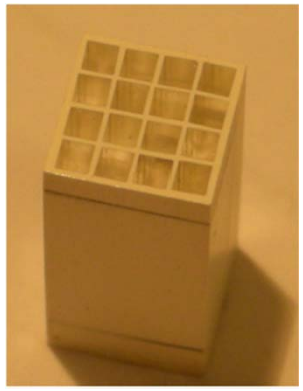

4x4 array of 0.96 x 0.96 mm^2 LYSO

G.Llosa et.al., 2008 IEEE NSS/MIC Conference Record

Continuous Crystal with SiPM Readout

13.2x13.2x10 mm^3 LYSO

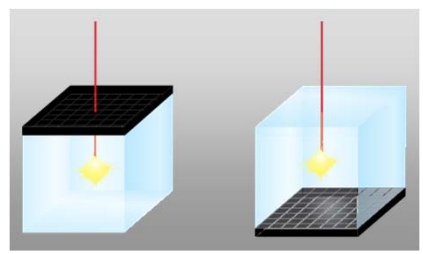

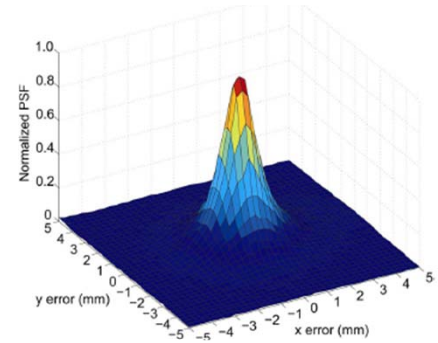

SensL 4x4 array of 3x3 mm^2 SiPMs

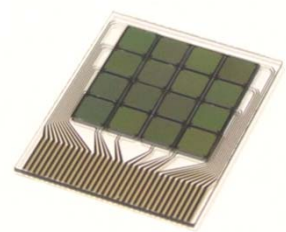

D.Schaart et.al., Phys. Med. Biol. 54 (2009) 3501-3512

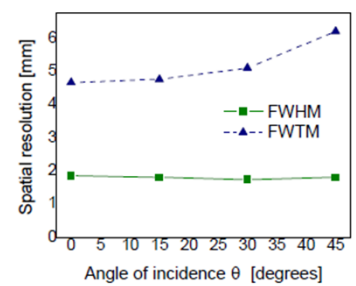

Spatial resolution with DOI correction

Simultaneous PET-MRI

Advantages of simultaneous PET-MRI

- MRI provides high spatial resolution for excellent anatomical information with good soft tissue contrast.
- PET provides extremely high sensitivity and specificity for studying metabolic activities and radiotracer uptake
- PET/MR delivers ~ ½ the radiation dose of PET/CT
- Simultaneous acquisitions result in perfectly co-registered images with less scan time than sequential imaging, and also allows time correlated studies such as in combination with fMRI

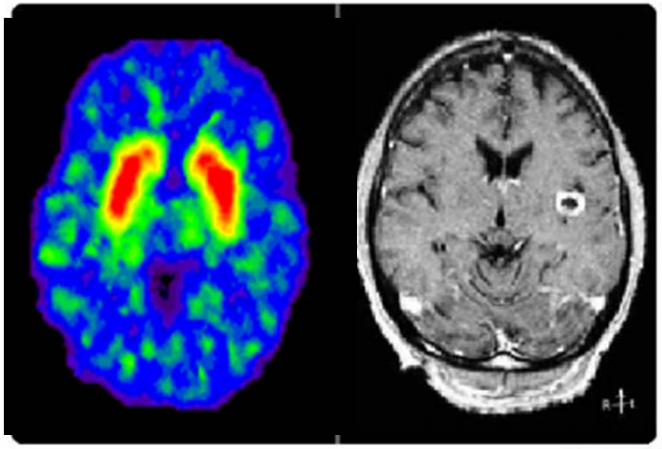

PET image MRI Image

What Are the Problems

- PMTs used in conventional PET detectors are very sensitive to even small magnetic fields
- MRI uses strong RF pulses at frequencies of several hundred MHz and pulsed gradient magnetic fields that can cause interference with the PET readout electronics
- PET detector and readout electronics can cause interference with very sensitive MRI detectors for measuring weak MRI signals
- Any magnetic materials in the PET detector can perturb the very homogeneous magnetic field of the MRI and can cause distortions in the MRI image

Small Animal PET-MRI

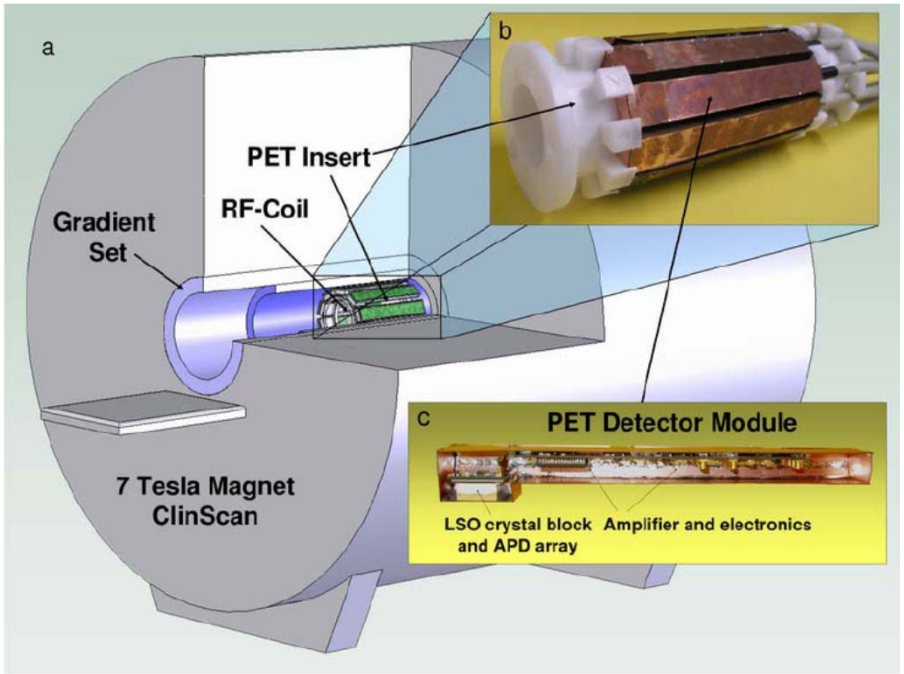

PET detector (APDs + preamps) is inside magnet but just outside RF coil

Requires extensive shielding and careful grounding to avoid pickup shielded

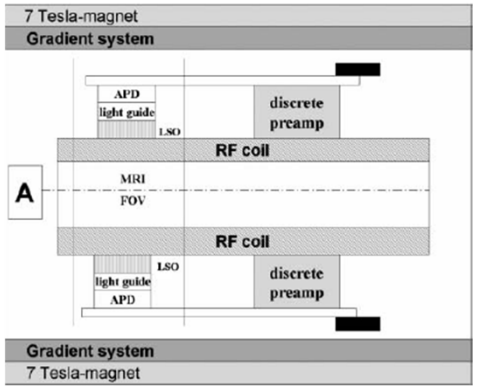

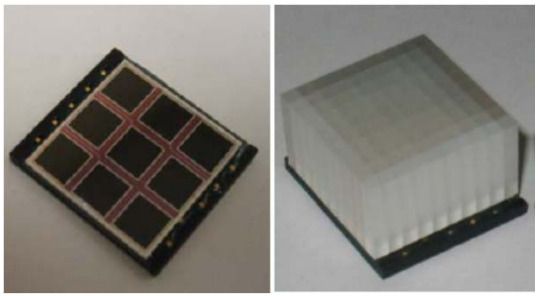

3x3 APD matrix 5x5 mm^2

10x10 LSO matrix 2.5x2.5x20 mm^3

10 Detector Blocks
38 mm dia x 19 mm axial FOV
Light sharing technique
Position resolution < 2 mm
Coincidence time resolution ~ 8 ns

B.Pichler, J. Nucl. Med. 2006 47:639-647
M.Judenhofer, PET-MR Workshop, Julich, 2008

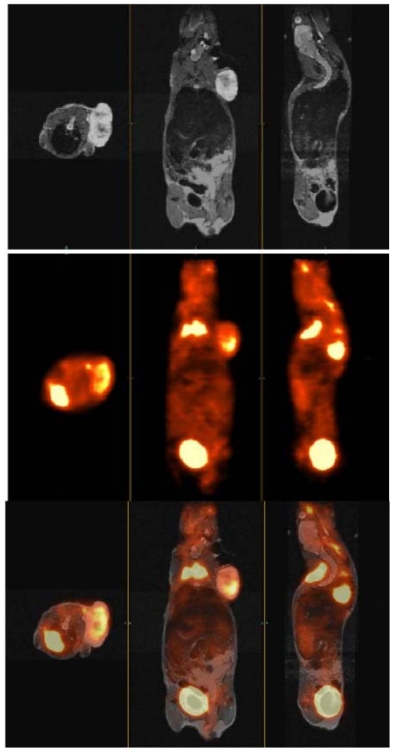

Whole body mouse image

PET-MRI with the RatCAP

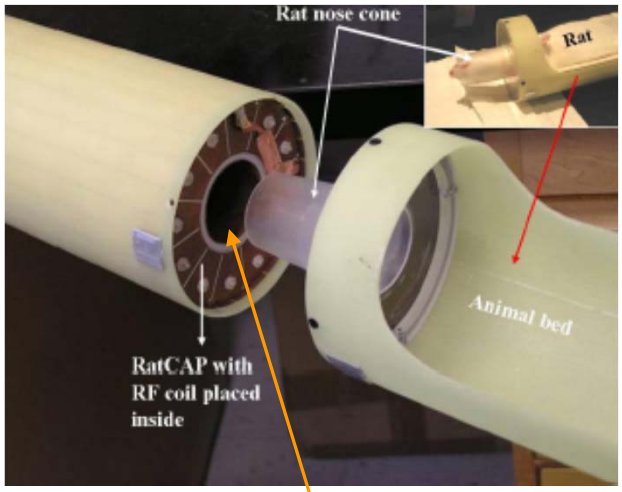

- RatCAP inserted in 9.4T small animal MRI
- Constructed from all non-magnetic components
- Coil placed inside RatCAP (within ~ 2 mm)
- Detector, electronics and cables all shielded
- Segmented shielding to reduce eddy currents

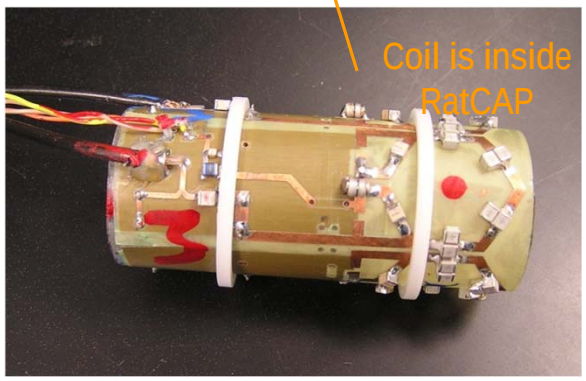

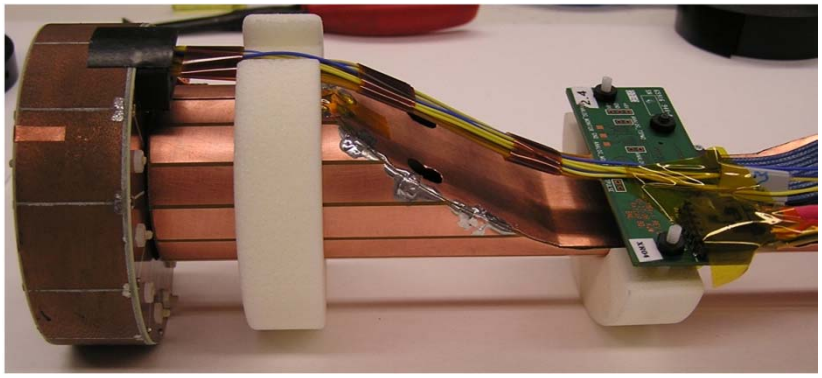

Rat brain image with ^{11}C-raclopride

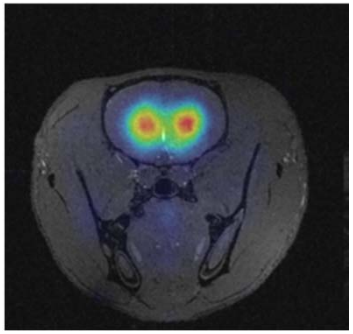

S. Maramraju, 2009 IEEE NSS/MIC Conference Proceedings

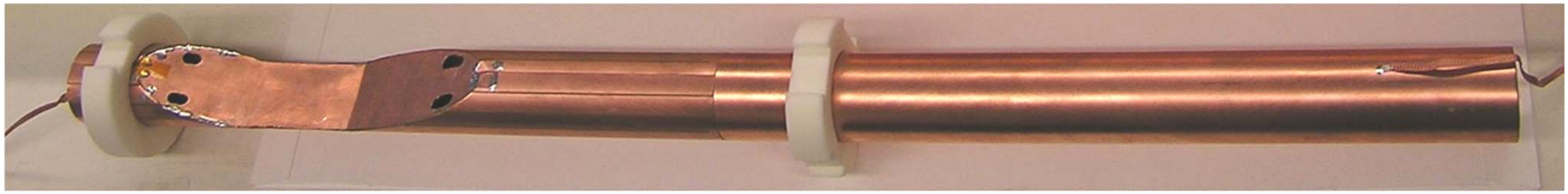

Human Brain PET-MR

Prototype Research System
MR/PET BrainPET* scanner

SIEMENS

3T Commercial MRI

MR Compatible PET Detector
36 cm dia x 10 cm axial FOV
3x3 APD matrix 5x5 mm^2
12x12 LSO matrix 2.5x2.5.20 mm^3
PET spatial resolution
- 2.5 mm (center) $\rightarrow$ 4.5 mm (r=10 cm)

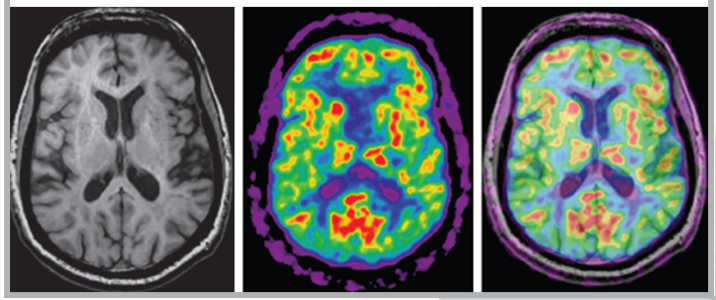

© Siemens Medical Solutions USA, Inc. – Molecular Imaging

* Works in Progress. The information about this product is preliminary. The product is under development and is not commercially available in the U.S. and its future availability cannot be ensured.

H.-P Schlemmer et.al, *Radiology*, Vol 248, No. 3, September. 2008

Summary

- Photodetectors are some of the most widely used devices in particle physics and nuclear medicine for detecting many types of particles (γ, e, h, ν,…)
- Photomultiplier tubes are still the most extensively used despite many of their limiting properties
- New solid state detectors are now achieving the same performance as PMTs in terms of gain and timing, and also work in magnetic fields, but have their own limitations in terms of area coverage, noise and radiation hardness
- Good overall detector design requires looking at all factors affecting performance (choosing the right photodetector, good light collection and matching, and low noise electronics)